VŠB - Technical University of Ostrava

Nanotechnology Centre

University Study Programmes - Nanotechnology

Master thesis

Incorporation of bio-metallic nanoparticles into fiber membranes and their future application

Inkorporace biosyntetizovaných nanočástic ušlechtilých kovů do vlákenných nosičů a možnosti jejich využití

Author Bc. Zuzana Konvičková

Supervisor Ing. Gabriela Kratošová, Ph.D.

Ostrava 2015

VŠB - Technical University of Ostrava
University Study Programmes
CNT - Nanotechnology Centre

Diploma Thesis Assignment

Student: **Bc. Zuzana Konvičková**

Study Programme: N3942 Nanotechnology

Study Branch: 3942T001 Nanotechnology

Title: Inkorporace biosyntetizovaných nanočástic ušlechtilých kovů do vlákenných nosičů a možnosti jejich využití
Incorporation of bio-metallic nanoparticles into fiber membranes and their future application

Description:

Aim of the master thesis is the preparation of gold and silver nanoparticles via biosynthesis and their incorporation into fibrous materials. Characterization of bionanocomposites and comparison of different types of spinning quality is included. Furthermore, the evaluation of future utilization will be also discused.

Master thesis will include:

1. Review of recent literature concerning various types of fibrous material preparation procedures and further potential application of these systems with incorporated gold and silver nanoparticles.
2. Preparation (biosynthesis) and characterization of gold and silver nanoparticles.
3. Incorporation of bio-metallic noble nanoparticles to fibrous materials by available methods.
4. Evaluation of results with respect to further applications.

References:

1. ANDRADY, A. L., Science and Technology of Polymer Nanofibers, Wiley-Interscience; 1th ed. 2008. ISBN-10: 0471790591, ISBN-13: 978-0471790594.
2. CHANG, W.-M., C.-C. WANG, and C.-Y. CHEN, The combination of electrospinning and forcespinning: Effects on a viscoelastic jet and a single nanofiber. Chemical Engineering Journal, 2014. 244(0): pp. 540-551.
3. HUANG, Z.-M., et al., A review on polymer nanofibers by electrospinning and their applications in nanocomposites. Composites Science and Technology, 2003. 63(15): pp. 2223-2253.
4. SCHRÖFEL, A., et al., Applications of biosynthesized metallic nanoparticles – A review. Acta Biomaterialia, 2014. 10(10): pp. 4023-4042.
5. KRATOŠOVÁ, G., VÁVRA I., HORSKÁ K., ŽIVOTSKÝ O., NĚMCOVÁ Y., BOHUNICKÁ M., SLABOTINSKÝ J., ROSENBERGOVÁ K., KADILAK A. and SCHRÖFEL A., Synthesis of Metallic Nanoparticles by Diatoms – Prospect and Applications. In: Rai, M & Posten, C. (eds): Green Biosynthesis of Nanoparticles – Mechanisms and Applications. CABI Publishing 2013, UK, (256 p.).

Extent and terms of a thesis are specified in directions for its elaboration that are opened to the public on the web sites of the Nanotechnology Centre.

Supervisor: **Ing. Gabriela Kratošová, Ph.D.**

Date of issue: 20.10.2014

Date of submission: 15.05.2015

prof. Ing. Jaromír Pištora, CSc.
Head of Department

prof. Ing. Petr Noskievič, CSc.
Vice-rector for Study Affairs

AUTHOR DECLARATION

The work submitted in this diploma thesis is the result of my own investigation, except where otherwise stated.

It has not already been accepted for any degree, and is also not being concurrently submitted for any other degree.

Ostrava, 15.5.2015 _____

Bc. Zuzana Konvičková

DECLARATION

- I was aware of the fact that my diploma work is fully covered by the Act No.121/2000 Coll. Copyright Act, particularly §35 - use of the work within the civil and religious ceremonies, in university performances and school use of the work and §60 – schoolwork.
- I acknowledge that the VŠB-Technical University of Ostrava ("VŠB-TUO") has the unprofitable right to use this diploma thesis (§ 35 paragraph 3).
- I agree that the thesis will be electronically deposited in the Central Library of VŠB-TUO for examination and a copy will be kept by the supervisor of the master thesis. I agree that the information about qualifying work will be published in the information system of VŠB-TUO.
- It was agreed with VŠB-TUO, in case of university interest, I conclude a contract with permission to use the work in accordance with §12 paragraph 4 of the Copyright Act.
- It was agreed that use this work; diploma work or to provide the license to other utilization I can do only with the approval of the VŠB-TUO, which is authorized to demand an adequate fee for the costs, which were expended to the creation of this work incurred by VŠB- TUO (until the actual amount).
- I agree that the submission of my work will be published in accordance with Act No.111/1988 Coll., about universities and the amendment of other Acts (Higher Education Act), regardless of the outcome of its defense.

Ostrava, 15.5.2015 _____

Student's name

Bohuslava Martinů 812, Ostrava - Poruba 708 00

_____

Address

ABSTRACT

This diploma thesis is focused on polymer fibers with incorporated silver and gold biosynthesized nanoparticles prepared by different spinning methods – centrifugal spinning and electrostatic spinning (Nanospider^{TM} technique). Theoretical part offers a brief introduction to a polymer world and introduces certain polymers often used in the spinning applications and their characteristics. Description of fiber spinning methods is included. Experimental part comprises all data about bio-metallic nanoparticles preparation and characterization by Transmission Electron Microscopy (TEM), X-Ray Diffraction (XRD), Atomic Emission Spectroscopy (AES-ICP), Infrared Spectroscopy (FTIR) and size distribution methods. Fibrous samples obtained by spinning methods are characterized by Scanning Electron Microscopy (SEM), TEM and FTIR. The efficiency of used spinning methods is compared and the quality of fibrous samples with incorporated nanoparticles is discussed. Additionally, antimicrobial properties of biosynthesized silver and gold nanoparticles are confirmed by antimicrobial evaluation.

Reference format:

KONVIČKOVÁ, Zuzana. 2015. *Incorporation of bio-metallic nanoparticles into fiber membranes and their future application*. Ostrava, 86 p. Master thesis. VŠB-Technical University of Ostrava. Supervisor Ing. Gabriela Kratošová, Ph.D.

ABSTRAKT

Diplomová práce je zaměřena na přípravu a vlastnosti biosyntetizovaných stříbrných a zlatých nanočástic zabudovaných v polymerních vláknech pomocí vybraných zvlákňovacích metod, a to odstředivým a elektrostatickým zvlákněním (technika Nanospider^{TM}). Teoretická část se zabývá vlastnostmi vybraných polymerů, které jsou v praxi hojně využívány při přípravě vláken. Dále je uveden přehled různých v současnosti využívaných zvlákňovacích metod a jednotlivé metody jsou stručně charakterizovány. Experimentální část podává informace o přípravě a charakterizaci biosyntetizovaných nanočástic stříbra a zlata a zvlákněných vzorků. K analýzám byly využity následující metody: TEM, SEM, XRD, ICP-AES, FTIR a hodnocení velikostní distribuce nanočástic. Využitelnost zvlákňovacích metod a výsledných vzorků se zabudovanými nanočásticemi je rovněž diskutována. Navíc byly testovány antimikrobiální účinky připravených nanočástic pomocí stanovení minimální inhibiční koncentrace a diskového difuzního testu..

ACKNOWLEDGEMENT

First, I would like to thank my supervisor Ing. Gabriela Kratošová, Ph.D. for her advices, comments and working meetings in very friendly atmosphere.

Many thanks to Ing. Jaroslava Morávková, Ph.D. (Pardam, s.r.o., Czech Republic) and Ing. Petr Mikeš, Ph.D. (Technical University in Liberec, Czech Republic) for their patience and kindliness during my educational stays. Moreover they provided me basic knowledge I needed in polymer science.

I would like to propose my thanks to Mgr. et BcA. Adam Schröfel, Ph.D. from Institute of Cellular Biology and Pathology (Charles University in Prague, Czech Republic), whose thoroughgoing comments were helpful.

I am grateful to people interested in characterization methods used in my work:

- antibacterial assessment: Mgr. Kateřina Rosenbergová, Ph.D., National Institute for Nuclear, Chemical and Biological Protection (Czech Republic) and Mgr. Kateřina Dědková, Nanotechnology Centre (VŠB - Technical University of Ostrava, Czech Republic)
- TEM analysis: Ing. Ivo Vávra, CSc., Institute of Electrical Engineering (Slovak Academy of Sciences in Bratislava, Slovak Republic) and Mgr. et BcA. Adam Schröfel, Ph.D., Institute of Cellular Biology and Pathology(Charles University in Prague, Czech Republic)
- SEM: Ing. Gabriela Kratošová, Ph.D., Nanotechnology Centre (VŠB - Technical University of Ostrava, Czech Republic)
- ICP-AES: prof. Ing. Jana Seidlerová, CSc., Nanotechnology Centre (VŠB - Technical University of Ostrava, Czech Republic)
- XRD: doc. RNDr. Edmund Dobročka, CSc., Institute of Electrical Engineering (Slovak Academy of Sciences in Bratislava, Slovak Republic), Mgr. Kateřina Mamulová - Kutláková, Ph.D., and Bc. Vladimír Foldyna, Nanotechnology Centre (VŠB - Technical University of Ostrava, Czech Republic)
- FTIR: Mgr. Pavlína Peikertová, Ph.D., Nanotechnology Centre (VŠB - Technical University of Ostrava, Czech Republic)
- Size distribution: Ing. Martin Žídek, Ph.D., Bulk Laboratory (VŠB - Technical University of Ostrava, Czech Republic)

- English corrections: Bc. Marek Krygel, Nanotechnology Centre (VŠB - Technical University of Ostrava, Czech Republic)

I would like to express thanks to my family without whose support I would not be where I am today.

Many thanks to my great classmates for the memories and experiences I would share with them during our studies.

CONTENTS

KEYWORDS

biosynthesis; diatom; *Diadesmis gallica*; nanoparticles; gold; silver; bionanocomposite; antimicrobial agent; minimum inhibition concentration, nanofibers, electrospinning, Nanospider™, centrifugal spinning, Forcespinning®, poly(vinyl alcohol)

LIST OF ABBREVIATIONS

CNT = carbon nanotube

DMF = dimethylformamide

FTIR = Fourier Transform Infrared Spectroscopy

ICP-AES = Inductively Coupled Plasma Atomic Emission Spectroscopy

MAA = methacrylic acid

MMA = methyl methacrylate

MW = molecular weight

NPs = nanoparticles

PA = polyamide

PAN = poly(acrylo nitrile)

PANI = poly(aniline)

PBT = poly(butylene terephthalate)

PC = polycarbonate

PCL = poly(ε-caprolacton)

PE = polyethylene

PEG = poly(ethylene glycol)

PEO = poly(ethylene oxide)

PGA= poly(glycolide)

PLA = poly(lactic acid)

PLGA = poly(lactic-co-glycolic acid)

PMMA = poly(methyl methacrylate)

PTFE = poly(tetrafluorethylene)

PUR = polyurethane

PVA = poly(vinyl alcohol)

PVDF = poly(vinylidene fluoride)

PVP = poly(vinyl pyrrolidone)

SEM = Scanning Electron Microscopy

TEM = Transmission Electron Microscopy

TEOS = tetraethyl orthosilicate

XRD = X-Ray Diffraction

1. INTRODUCTION

In the middle of the last century it was not obvious that we were able to control matter at the atomic or molecular level. Especially Schrödinger's idea said that atoms cannot be localized in space accurately, because they are not considered as individualities which can be identified [1]. At the end of 50' in 20^{th} century some scientists predicted the construction of "molecular machines" as same as nature does. The primary concept of nanotechnologies was presented by Richard Feynman, an American physicist, scientist and Nobel prize laureate in physics, in his memorable lecture called "There's plenty of room at the bottom" at the American Physical Society meeting at California Institute of Technology [2]. He allowed the possibility of manipulating with tiny objects – nowadays in nanoscale (10^{-9} m). An eventuality of using the properties of nanometric building components can be used in many areas such as material engineering [3], chemical industry [4], electronics [5], optical systems [6, 7], but this branch also became interesting in biomaterial research and its applications in medicine [8], pharmacy [9] and biotechnology [10]. Thus, the new interdisciplinary field – nanotechnology – is here.

Nanotechnology comprises a research and technology development on the atomic, molecular or macromolecular levels in the range of 1-100 nm. Nanotechnology is also considered as the science creating and using structures, devices and systems, which dispose of new features and functions due to their small or intermediate sizes [11]. These structures have new unique chemical, optical, electrical, mechanical or thermal properties [12-14]. However, these effects can become significant when the aforementioned nanometre size is reached. For example, the increase in surface area to the volume ratio dramatically changes mechanical, thermal and catalytic properties of nanomaterials [15].

There are two basic approaches to produce materials or structures in nanoscale: top-down or bottom-up**.** Top-down method reduces "large" pieces of materials all the way down to the nanometric sizes. This approach demands larger amounts of materials and can lead to a large energy consumption during experiment or working process and be time-consuming. The bottom-up methods can create products by building them up from the atomic- and molecular-scale components, which can have disadvantages as same as the top-down methods [16].

Methods for the preparation of nanomaterials or nanostructures can be also classified into physical or chemical type. Both physical and chemical methods have many advantages but certain limitations too. Thus, it is important what kind of material will be prepared,

which properties initial materials have and what type of instrumental equipment is available. All these points are closely linked with possible application in market and financial resources. Physical branch covers material preparation when the particular physical process is used. This field may include e.g. physical vapor deposition (PVD) [17], pulse laser deposition (PLD) [18] or sputtering [19], often used for thin film preparation. On the other hand, chemical methods utilize chemical processes and synthesis, e.g. sol-gel methods [20], co-precipitation [21] or intercalation [22]. Common disadvantage in material production is the use of toxic chemicals and the creation of reactive intermediates, thus it instigates the environmental hazard [23].

Biosynthesis is a special case of chemical methods. The application of biological reactions and processes in living organisms contributes to the formation of nanomaterials, especially of metal nanoparticles [24-27]. In this method chemicals (metal precursors) play a role only as providers of initial compounds for making the material. This “bio” branch and bionanotechnology as an individual research field are often determined as environmentally friendly. Furthermore what is a great asset of this branch, it is undemanding to initial financial investments and an acquisition of biomass is easy and cheap [28, 29].

One part of this thesis is a preparation of silver and gold nanoparticles using brown algae called diatoms. According to the previous results [30] these nanoparticles showed antibacterial properties against chosen bacteria cultures. Moreover, this kind of bionanocomposite with only gold nanoparticles have other interesting properties such as successful catalytic activity in oxidation of carbon monoxide [31] or warfare agents hydrolysis[32].

Why the term bionanocomposite? Diatoms are unicellular organisms whose body is enclosed in silica box called frustule [33]. A frustule (the siliceous matrix) provides an excellent place for the formation of nanoparticles and subsequent attachment. Through the frustules a wide range of reducing functional groups are present. These groups are responsible for nanoparticle formation: reduction of metallic ions and stabilization of the nanoparticles on the silica surface in one step. Stabilization is also provided by substances of an organic origin and does not require utilization of additional surfactants [24, 34].

In this work, the main goal is an incorporation of biosynthesized metallic nanoparticles to polymer fibers. Two spinning techniques for polymer fiber formation were used:

centrifugal spinning and electrospinning. Centrifugal spinning technique was carried out in Pardam company in Nové Město na Moravě. Electrospinning process was performed in Technical University in Liberec in Department of Nonwovens and Nanofibrous materials.

Gold and silver nanoparticles will be used in the form of bionanocomposite (as was mentioned above) and in nanoparticles suspension too. In this case nanoparticles are not attached on the diatom surface only but also released to a solution obtained from biosynthesis process. Because of antimicrobial properties of silver and gold nanoparticles the final polymer fibers (with nanoparticles inside or on the surface) may be used in several applications as filtration systems or as a membrane part of respirator.

2. THEORETICAL PART

2.1 Biosynthesis: a simple method for metallic nanoparticles preparation

Because of biosynthesized origin of metallic nanoparticles in the experimental part a short chapter about biosynthesis is included.

The biosynthesis classified into a special case of chemical methods is a process which takes place in the presence of different type of biomass as bacteria [35, 36], fungi [37, 38], algae [39, 40] or high plants and their extracts [41-43] because these types of organisms can be easily cultivated or harvested. More specific biosynthesis uses biological processes occurred inside the chosen living biomass. Therefore, biosynthesis is considered as a low-cost and environmentally friendly method of nanomaterials production [15, 28, 44, 45].

We can distinguish two types of biosynthesis: extracellular and intracellular.

Extracellular biosynthesis takes place on the cell surface. The cell surface is rich in a wide range of the functional groups such as carboxyl (-COOH), amino ($-NH_2$) or hydroxyl (-OH) which are bound in more complicated compounds such as amino acids, proteins or polysaccharides. That is an important fact in biosynthesis research; functional groups reduce gold (Au^{3+}) or silver (Ag^{+}) ions from their aqueous solutions to zero valent form. Metal ions (gold which forms the tetrachloroauric complex $[AuCl_4]^-$ in aqueous solution and silver in the form of Ag^{+}) adhere to the cell surface near the charged groups (e.g. amino group) [46]. After the fast adsorption of metal ion to the cell wall, the second stage – bioreduction – occurs [46, 47]. The formation of metallic nanoparticles is clearly seen as a color change in the solution. The solution becomes purple for gold nanoparticles and yellow-brownish for silver ones [48] (see Figure 1).

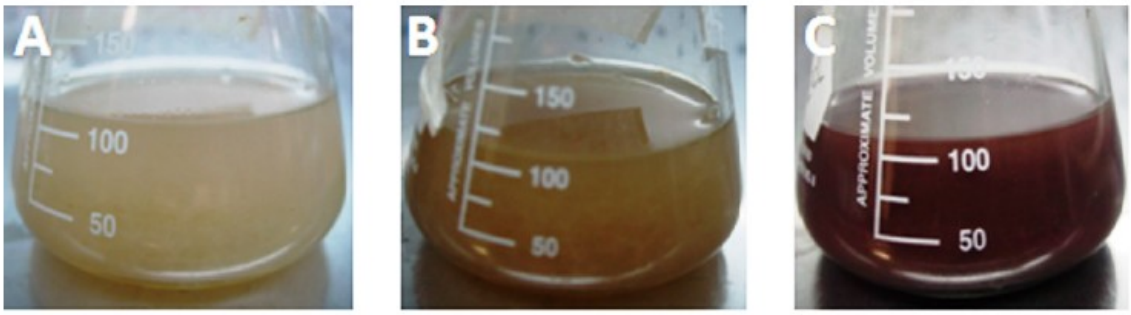

Figure 1: The color changes after supplementation of precursors. Biosynthesis with fungus *Neurospora crassa*: (A) fungus culture without precursors; (B) fungus culture after 24 hours in $AgNO_3$; (C) fungus culture after 24 hours in $HAuCl_4$[25]

For example in biosynthesis of gold nanoparticles using foliar broth (randomly selected plant leaves), the role of biocompounds as flavonoids and reducing sugars is

confirmed. In the redox reaction the polyols as well-established reductants would serve as the principal electron donor [49]. On the other hand silver nanoparticles synthesized with latex of *Jatropha curcas* are reduced and stabilized with cyclic peptides curcacycline A and curcacycline B [50].

Intracellular biosynthesis takes place inside a chosen microorganism, for example bacteria. Genus *Rhodococcus* spp. is widely used in industrial applications for biodegradation of organic compounds or in bioremediation [51]. This type of bacteria is also suitable for biosynthesis of silver nanoparticles with antimicrobial properties [52] as well as for gold nanoparticles synthesis with size distribution 5 - 15 nm [53]. Intracellular biosynthesis of metallic nanoparticles can take place in presence of enzymes, including the transport of ions into the cell and the formation of particles [23, 40].

2.2 Polymers as materials for fiber production

Polymer are widely used in material engineering [54], medicine [55] or biotechnology [56]. One important field where polymers play a major role is nanotechnology, especially in the preparation of polymer fibers and nanofibers. Given the importance of fibers and nanofibers a brief overview of basic polymer properties will follow in this chapter.

2.2.1 Brief introduction to a world of polymers

A polymer is a large molecule built up by repetitive bonding together of many smaller units called monomers [57]. These features relate with molecule size and are associated with fundamental built units – we can distinguish inorganic or organic compounds.

Characteristic properties of macromolecular compounds are closely related to the size of their molecules. Monomer units and their repetition cause an increase in molecular weight (MW). MW of the most commercial polymers dispose of values between 40 000 – 200 000 [58], for example ultra high molecular weight polyethylene (UHMWPE) have a MW in the range 1-6 million. MW for greases and soft waxes range between 500 and about 3000, whereas some tough and brittle waxes have MWs between 3000 and 10 000 [59]. When the intermolecular forces are high (for example polyamides), the material can gain sufficient mechanical properties at lower MWs [60].

An increasing MW is a major aspect in continuous changes of low-molecular compounds, especially volatility, diffusion etc. On the other hand, polymer can have some characteristics of macromolecules as a swelling in a solvent; polymer is solved in a solvent with its increasing volume. Another aspect in which a relative MW plays a major role is a synthesis of certain types of polymers. Macromolecules consist of 10^3 and more atoms. They can be joined into unwanted structure isomers with different chemical or physical properties [61]. It is difficult to control the growth of the molecules which results in molecules of various lengths and therefore varying MWs [60].

An ability of atoms to assembly into macromolecules is given by the capability to create two chemical bonds at least. Thus a low - molecular compound – a monomer must contain certain functional groups as - OH, - COOH, - CHO etc. [61].

The polymers may be found in various physical states: crystalline, glassy, rubbery and plastic. Phase transitions are given by melting point T_m and glass transition temperature T_g [61, 62]. T_g is defined as the change of an amorphous material from solid

(glassy) to a liquid (rubbery) state [63]. Both states of amorphous material are non-equilibrium states, glassy state of polymer can be described as a metastable solid state. A rate of changes of amorphous material is different and is time-dependent. It is caused by the ability of molecules inside the material to respond to changes in their surroundings. Movement of the molecules in a system is greatly reduced in the glassy state in comparison with the rubbery state [64]. Thus, the phase state depends on its composition, temperature and time of an amorphous material and reflects changes in molecular mobility [65]. According to Figure 2 the enthalpy of a material changes differently with the temperature in the glassy and rubbery states.

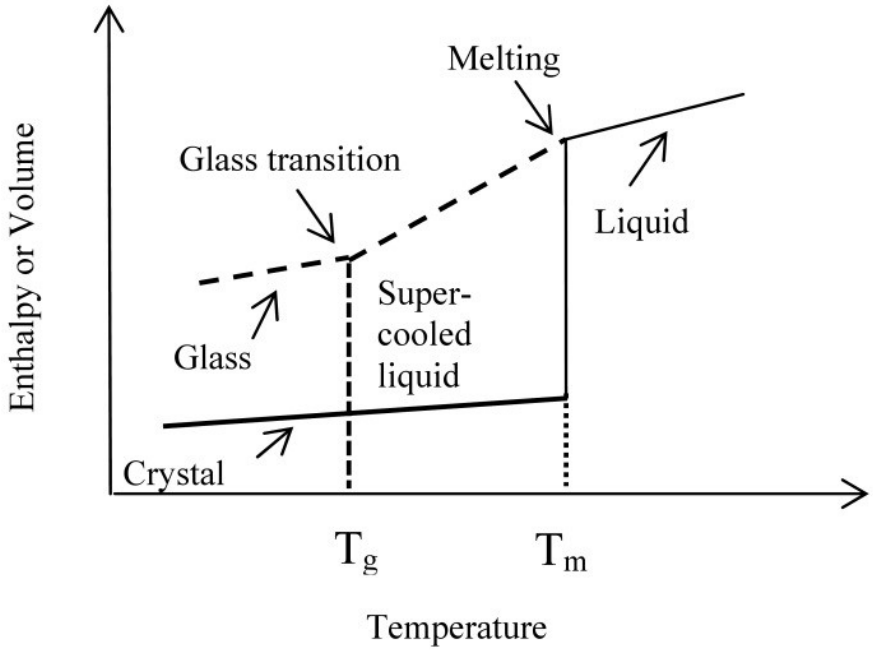

Figure 2: Various physical states of polymers affected by an increasing temperature [62]

If the liquid is cooled the kinetic energy of atoms is reduced. Molecule of a liquid phase becomes a part of the growing crystal its spatial position is fixed and molecule loses its free motion. Sometimes macromolecular substances behave like low - molecular compounds which crystallize from solution during cooling of the melt. An ability of crystallization is usually determined by sterically regular structure of the polymer chain. A crystallization of a polymer with spatially disordered structure does not occur but the polymer changes its structure through aforementioned states [61].

Polymer solutions are very different from the ideal solutions. With a few exceptions, the linear polymers are not dissolved immediately but first swelled. The polymer swelling is caused by the solvent diffusion into the polymer and it is accompanied by a subsequent

increase of its volume. However the presence of a crystal lattice in the crystalline polymers makes dissolution harder. The dissolution process depends on the degree of interaction between the macromolecules and solvent molecules and is controlled by the law of thermodynamics. Dissolution of polymers is a slow process whose rate decreases with an increasing degree of polymerization. The whole process of swelling does not always reaches complete dissolving.

Complete dissolution is not possible in the case of cross-linked polymer [61]. The cross-linking is a mutual linking of one polymer chain to other to large macromolecules. Just a small amount of cross-linking agent is sufficient to be insoluble in a certain solvent. The necessary amount of cross-linking agent decreases, when molecular weight increases. Cross-linking leads to enhanced insolubility, fusibility, heat-resistance or resistance to chemicals [61].

2.2.2 Classification of polymers

According to the literature [61] polymers can be classified into several groups:

- biological polymers or biopolymers (proteins, nucleic acids, etc.),
- fibrous materials (cellulose, silk),
- natural polymers (rubber, collagen, gelatin),
- synthetic polymers,
    - plastics,
    - chemical fibers (polymer fibers),
    - polymer coatings.

Based on the different structural arrangement, there are two types of polymers:

- amorphous,
- crystalline.

A random structural arrangement is typical for amorphous polymers. However in the case of crystalline polymers, specific places with highly ordered and structured character are present. These regions are often called crystallites.

Any polymer cannot be completely crystalline. There are always areas where the molecules are found in random arrangement. Polymer may be considered as semi-crystalline material with amorphous regions, because a part of molecules may be present in

the amorphous areas and the rest in the crystallites. The degree of crystallinity is determined relative to the amount of crystals present in the sample.

The nature of the polymer, whether it is amorphous or partially crystalline is an important fact for industrial applications. The geometric regularity of the polymer arrangement of the groups in the main chain, and intermolecular forces predetermine polymer for certain applications. Moreover, a significant point is a ratio between the degree of crystallinity and MW as it is seen on Figure 3. This graph describes the utilization of poly(ethylene) (PE) based on aforementioned relationship. PE is typically used more in soft waxes and greases at low values in MW as well as crystallinity. On the other hand high MW and highly crystalline materials are often used as hard plastics [60].

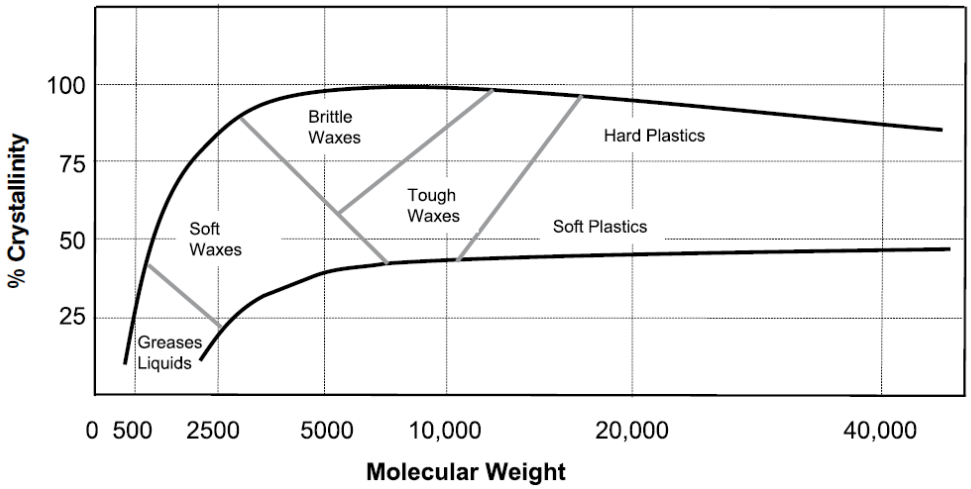

Figure 3: Molecular weight and crystallinity: effects on the properties of PE [59]

Polymer materials can be classified by their method of synthesis, too [57]. Chemical reactions can be divided into two groups:

- a step - growth reaction,
- a chain - growth reaction.

Step - growth polymers (nylon or polyesters) are produced by reactions in which each bond in the polymer is formed independently on the others. Most step - growth polymers are produced by a reaction between two difunctional reactant [57].

Chain-growth polymers are produced by chain - reaction polymerization in which an initiator contributes to a carbon - carbon double bond (a vinyl monomer) to yield a reactive intermediate. This intermediate reacts with a second molecule of monomer to a new

intermediate. New intermediate also reacts with a third monomer unit and a reaction continues step by step.

Another sorting is closely linked with previous classification and is also related with methods of preparation but in different way:

a) polyaddition.
b) polycondensation,

In the addition polymerization process, a catalyst initiates the polymerization reaction and each monomer adds onto the next polymer until all the monomers are polymerized (Figure 4). A common example of an addition polymer is PE. PE is polymerized from ethylene monomer, which is a gas at room temperature. The double bond in the ethylene molecule is broken and a bond with an adjacent ethylene molecule is formed. The result is a large molecule with high MW [60].

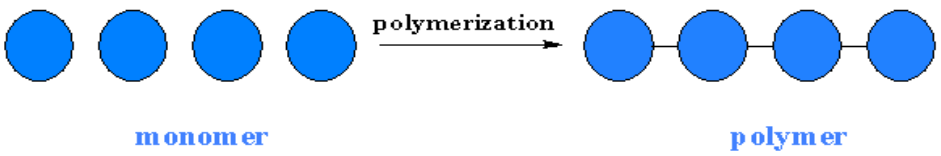

Figure 4: Polymerization process [60]

In the condensation polymerization, each monomer adds onto the next monomer too, but this chemical reaction also produces a low-molecular weight byproduct that has to be continuously removed out of the system. Condensation polymers are usually polymerized from two or more families of monomers. Nylon and polyesters are examples of condensation polymers.

2.3 Polymer fiber and nanofiber preparation

Polymer nanofibers have a diameter in the order of tens of nanometers to one micrometer, often from 50 to 500 nm [54]. With respect to the definition of nanoscale objects in the term of their size (the range of 1 – 100 nm), in the following text a term fiber will be used.

According to utilized material the various types of fibers exhibit interesting characteristics such as high surface area per unit mass, high porosity, structural mechanical properties or flexibility. A choice of initial polymer solution [66, 67], co-processing polymer mixture [68] or melts [69] can provide ways to control chemical composition and the nature of fibers, which is closely linked with their final properties [54, 70].

2.3.1 Fiber preparation via electrospinning

The process of spinning in the presence of an electrostatic field has been known since the 16th century [71], but the first work engaged in spinning theory of fine fibers was written at the beginning of 20th century by William J. Morton [72]. Another crucial work of modern capillary electrospinning is the work of Czech – American scientist John Zelený, who designed the capillary apparatus for the study devoted to electrical discharges of liquid points [73]. Unfortunately, acquired knowledge did not have large industrial applications and this topic was not developed. Why? One reason could be that there was a lack of optical and analytical instruments for objects studying in the micrometer even though in nanometer scale. In addition, the first prototype of electron microscope was designed in 1931 [74]. Almost sixty years later, in the 80', an industrial potential of fibers was developed.

An important discovery in the field of polymer fiber preparation was the construction of a unique technique called Nanospider^{TM}, which allows the production of fibers with diameters from 200 to 500 nm. Nanospider was patented by Czech scientist Oldřich Jirsák from the Technical University in Liberec [75]. In cooperation with Elmarco company this electrospinning device produces fibrous materials in sizes larger than 1 m are for commercial uses and applications.

Electrospinning is a non-mechanical, electrostatic technique involving the use of high voltage electrostatic field to charge the surface of the liquid solutions (especially polymers). Electric potential is applied between the polymer solution and a grounded collector. Due to this process the drops of polymer are drawn and as the electric field

overcomes the liquid surface tension charged jet is ejected. The path of charged jet is controlled by an electric field (Figure 5) [67].

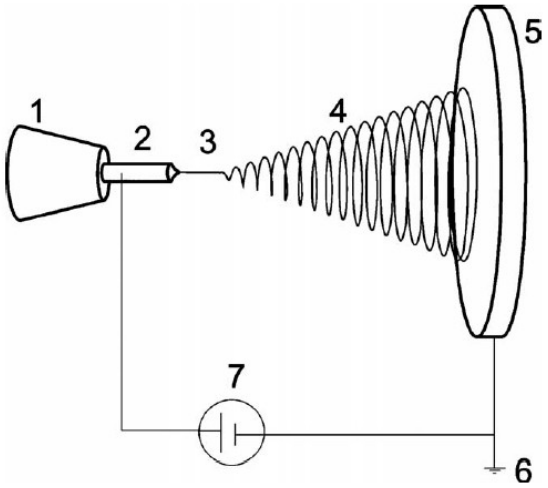

Figure 5: An instrumental equipment for electrospinning process: (1) - (2) spinneret, (3) stable part of liquid jet, (4) Taylor cone, (5) - (6) grounded collector, (7) high voltage supply [67, 76]

Electrospinning includes a wide range of physical phenomenon classified as electrohydrodynamics. This field studies, for example, the principles of electrophoresis, electroosmosis or electrodifusion. Without any influence of the external electrostatic field the liquid surface shows surface tension resulting from the effect of short intermolecular forces. This phenomenon is associated only with the liquid surface whose thickness is comparable with the intermolecular forces range. However, the external electrostatic field begins to effect on the liquid surface the charges are induced [67].

Electrospinning technology can be divided into two groups, depending on the place from which the fibers are taken out. The first group is a capillary electrospinning, but this technique is limited by the amount of the injected polymer and it is less productive. Recent techniques are oriented to highly productive processes of the fiber production from the free surface of the polymer by self-organization process. This method is referred as needleless [67].

2.3.1.1 Parameters affecting fiber appearance

Important parameters for the polymer fiber preparation are for example: MW, polymer structure in the term of polymer branching, as well as a viscosity, conductivity, surface tension and further parameters such as flow velocity, concentration of polymer solution, distance between spinneret and the collector or temperature and humidity [67].

As it was said before the concentration of the polymer is an important aspect in the process of spinning. If concentration is too low the final fibrous sample is a mixture of fibers and polymer defects in the form of beads. If the concentration rises, the shape of the droplet changes from spherical to spindle-like shape. Furthermore, an increasing or decreasing concentration is also closely linked to the viscosity of the polymer solution, which may determine fiber shape and their morphology during the electrospinning process. It was found out that a lower viscosity interrupts a continuous fiber formation. On the other hand high values of viscosity may cause ineffective ejection of the polymer from spinneret [66, 77].

MW of the polymer may influence the rheological properties or electrical such as conductivity or surface tension. Moreover, the low MW of the polymer can result to formation of larger droplets without fibers. On the contrary high MW can increase a diameter of electrospun fibers. Surface tension of the polymer solution contributes to the whole appearance of the fibers. This phenomenon is associated with solvents in which the polymer is dissolved. If the suitable solvent is chosen, the fibers may be obtained without defects. However, if high surface tension during electrospinning occurs, jet path is unstable and may generate sprayed droplets [77].

One of the important processing parameters is an applied voltage. Higher voltage causes greater stretching of the polymer solution due to higher Coulomb forces in the jet. This may lead to the fiber diameter decrease and to the fast evaporation of the solvent from the fibers [66, 77, 78]. Solvents used in the preparation of polymer fibers have a considerable effect on spinning, because the dissolution of the polymer in a suitable solvent is first step in the electrospinning process. Solvents dispose of certain properties such as good volatility, vapor pressure or boiling point. Rapid solvent evaporation and phase separation occurs during jet thinning. Solvent vapor pressure plays also an important role in determination of the evaporation rate and fiber drying. Widely used solvents are chloroform, ethanol, dimethylformamide (DMF), water or acetone and depend on the type of the polymer [77]. Electrospinning parameters are summarized in Table 1.

Table 1: Certain parameters important during electrospinning [77]

Solution parameters	viscosity	high increase in fiber diameter
	polymer concentration	increase in fiber diameter relative to concentration
	MW	reduction of beads with increasing MW
	conductivity	decrease in fiber diameter with increasing conductivity
	surface tension	high surface tension may cause an instability of the charged jet
Processing parameters	applied voltage	decrease in fiber diameter with higher applied voltage
	distance between the collector and spinneret	minimum distance is required for uniform fibers
	flow rate	generation of the beads with increasing flow rate
Ambient parameters	humidity	high humidity may result to a pore formation
	temperature	increasing temperature may cause fiber diameter reduction

2.3.1.2 Polymers widely used in electrospinning process

There are a large number of polymers suitable for electrospinning and which are capable for fiber forming with submicron diameters. Polymers can be both natural and synthetic origin, even though nucleic acids or polysaccharides [77].

Natural polymers are used in tissue engineering, filtration membranes or in various biomedical fields. Natural polymers exhibit a high biocompatibility and low immunogenicity compared with synthetic polymers. Often used polymers are: collagen, gelatin, chitin, casein, cellulose acetate or fibrinogen. For example, chitosan has good physico-chemical properties comprising a solid-state structure. Collagen scaffolds are often used in a wound dressing or tissue engineering where mimic native collagen network.

Gelatin is a natural polymer which is widely used in medical or pharmaceutical applications due to its biocompatibility and biodegradability in physiological environment. A drawback of natural polymer fibers may be partial denaturation, which may lead to the degradation of initial material during spinning process [77].

In the case of synthetic polymers, there is a number of materials suitable for electrostatic spinning. Frequently used polymer is poly(ε-caprolacton) (PCL), which has a great potential for example in the bone tissue engineering. PCL fibrous structure allows a proliferation, viability and cell adhesion because a high porosity and large pores enhance cell growth and osteointegration [79]. Moreover a mixture of PCL and gelatin improves

final properties of scaffold in the term of enhanced cell migration into the PCL mesh [80, 81].

The cell biocompatibility was also found in poly(lactic-co-glycolic acid) (PLGA) fibrous scaffold [82, 83]. PLGA is a suitable material for non-woven scaffolds because their porosity is higher than 90 % and high surface area enables effective cellular attachment alongside to the fiber orientation. These materials can be subsequently impregnated with antibiotics in reducing post-surgery adhesion [77].

Because of complex applications of fibrous structures a combination of two or more materials is often used. It deals with structural or mechanical properties, but also the pore size or morphology. For example, the elastic poly(ethylene-co-vinyl alcohol) (PEVA) is less flexible after adding of poly(glycolide) (PGA) [84]. Thermal stability of poly(methyl methacrylate) (PMMA) can be increased by co–polymerization with methyl methacrylate (MMA) and methacrylic acid (MAA) [85].

Polyurethanes are important materials for electrospinning preparation of fibrous membranes. In the case of affinity membranes an attachment of specific target molecules on the membrane surface occurs. In addition, affinity membranes give a great potential of removing organic components from waste water. For protein purification a polyurethane (PUR) or PMMA membranes are useful [86, 87].

Fine fibers from poly(ethylene oxide) (PEO) may dispose of crystalline domains, according to the fiber axis [88, 89]. Furthermore, crystallographic orientation of these electrospun fibers prepared from poly(vinylidene fluoride) (PVDF) or polyaniline can be also seen [78].

Following polymers are also involved in electrospinning process and their fibers have a various form of applications: nylon 6 in filtration systems [90], poly(acrylo nitrile) (PAN) as ion-exchange membranes in micro- or ultra-filtration systems [91], poly(ethylene glycol) (PEG) may serve as an encapsulation site in drug delivery [92] or poly(vinyl alcohol) (PVA) as a non-woven antibacterial membrane with silver nanoparticles [93].

In conclusion electrospinning provides fibrous polymeric materials widely used in medicine [79], biology [94], chemical engineering [91], or in protective clothing applications [95] (see Table 2).

Table 2: Chosen polymers suitable for wide range of application [58, 66, 77, 96]

Polymer	Abbreviation	Solvent	Application
Poly(ε-caprolacton)	PCL	Chloroform : methanol (3:1)	bone tissue engineering
Polyurethane	PU	DMF	nonwoven tissue template, wound healings
Poly(vinyl alcohol)	PVA	distilled water	wound dressings
Poly(ethylene-co-vinyl alcohol)	PEVA	toluene	nonwoven tissue engineering scaffolds
Nylon 6,6; PA-6,6	-	formic acid	protective clothing, filtration systems

2.3.2 Centrifugal spinning

An alternative technique for the fiber preparation (with diameters from 150 nm to 3 μm) is a centrifugal spinning, so called rotary jet spinning or forcespinning. This technique operates using centrifugal force to extend the fibers from the spinning unit [97]. Due to this method a number of different spun fibers increases. Moreover, fiber mass production is more effective, the cost to fiber preparation is reduced and environmental risk becomes lower. Wide utilization of certain materials greatly expands due to replacement of the electrostatic forces by centrifugal. This technique also provides spinning process of the conductive material to form fibers. If necessary, high temperature may be applied in the vicinity of spinning unit to melt the solid material and spun it without previous chemical preparation [98]. Moreover, centrifugal spinning allows the preparation of fibers from solutions of higher concentrations than electrostatic spinning [99].

Centrifugal spinning apparatus consists of a spinning unit which contains a liquid (polymer solution or melt). When spinneret rotates around its axis and a rotation speed is determined, a viscous jet is ejected. Then jet drops on metal collector wherein the fibers are formed (see Figure 6). In the case of polymer solutions a solvent is evaporated during the jet path [97].

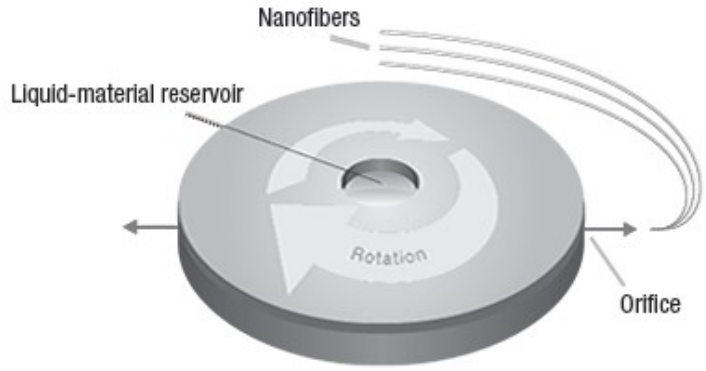

Figure 6: A scheme of centrifugal spinning apparatus [100]

Whole spinning process is divided into three stages: initiation jet, jet extend and solvent evaporation. During the first step the critical rotational speed for the jet ejection is reached. Very important parameters, which influence a jet extension are the viscosity of the liquid and angular speed. These two parameters significantly affect the character of the spun fibers. When both viscosity and angular speed are large enough continuous fibers with a minimum number of defects are formed. If solution viscosity is reduced, it is necessary to increase the angular speed. If both viscosity and angular speed are decreased, the fibers are still spun, but with a certain number of beads or other defects. These defects are formed, because the centrifugal forces are not able to overcome the surface tension and the jet path is prolonged. A third case may occur when angular speed and viscosity are too small, thus no fibers are formed [97].

Initial polymer solution plays an important role in determining the morphology and structure of centrifugally spun fibers. Especially it is rheological behavior, surface tension, MW, polymer concentration, solvent type or solvent vapor pressure. Generally, MW, solvent, solution concentration and possible additives in the solution affect together the spinning process in the term of structural changes and surface tension of the solution. Centrifugal forces must overcome the surface tension. Then the liquid jet is extended.

In the case of the experiment with the PAN polymer it has been found out when less than 6 % wt PAN concentration is spun no fibers are formed. If the concentration rises to 8 % wt fibers are formed with beads. The ideal concentration for the PAN fibers ranged between 10 - 15 % wt. It was found out that increasing solution concentration causes larger fiber diameters. A fiber formation is a function of polymer concentration. Optimum range of solution concentrations increases a probability of fiber formation [99].

In the case of a centrifugal spinning an important factor is the effect of spinneret rotational speed. Higher centrifugal force may cause the greater extension and thinning of polymer jets resulting to fiber. Average fiber diameters may be decreased with increasing speed. Fiber structure may be also affected by nozzle diameter. Small nozzle diameter may lead to volume reduction of extended polymer. The last important parameter is the distance between the collector and the spinning unit, because a minimum distance to the solvent evaporation must be determined [99].

Centrifugal spinning provides a large number of spun materials such as PEO [98], PC [101], PCL [102], PLA [101], PVP [55, 103] and others [98]. Centrifugal spinning focuses on applications in tissue engineering, for example poly(lactide acid) (PLA) is suitable material as scaffolds with controlled surface roughness [104]. PCL or poly(vinyl pyrrolidone) (PVP) may serve as drug delivery vehicles [105]. Moreover, PVP-based iodine fibers may be used as highly porous mat structure with antibacterial properties against chosen bacteria cultures. These properties provides biocide iodine incorporated inside the fibers [55]. PVP may be also modified with another composite part such as silica. Tetraethyl orthosilicate (TEOS) was used as a precursor to prepare silica sol-gel precursor with PVP solution for centrifugal spinning. Final fibers may be used as multilevel structured silica material for drug delivery or nanofiltration [103]. Poly(butylene terephthalate) (PBT) fibers exhibited higher crystallinity and enhanced molecular orientation after centrifugal spinning [106]. PAN is stable polymer which can be used in tissue engineering, composites, sensing or serves as a precursor for the preparation of CNT [107].

In conclusion, centrifugally spun fibers have a wide utilization for example in tissue engineering [108], in the field of ceramic fibers [109] or carbon electrodes [110].

2.3.3 Applications of fibrous materials with incorporated particles

Many types of colloidal nanoparticles such as gold [111], zinc [112], titanium [113], or CNTs [114], and other particulate matters [115] may be incorporated into the polymer fibers, mixtures of polymers or co–polymers. With respect to the thesis experimental part a brief overview of various types of incorporated nanoparticles into the polymer fibers will follow.

In the most cases of hybrid nanocomposite preparation, nanoparticles are obtained by chemical and/or thermal synthesis. Then, nanoparticles are dispersed in the polymer solution, inserted into the spinning unit and spun together with the fibers simultaneously

with solvent evaporation [78]. There are several drawbacks of this approach such as non-homogenous dispersion of nanoparticles in the polymer matrix or an aggregation of nanoparticles. These limits may influence the uniformity of composite structure [116].

The other way may be a dissolution of metallic precursor together with the polymer and spun [117]. Then, manoparticles are synthesized directly in the solution for example during electrospinning process. Gold nanoparticles (Au) with sizes between 5 and 20 nm were directly obtained in the PVP solution using laser ablation and then the PVP/Au solution was electrospun into uniform fibers [111].

Also silver selenide nanoparticles were incorporated into PVP fibers. Selenide on the surface of silver nanoparticles provides a strong chemical interaction between nanoparticles and polymer. Moreover this hybrid nanocomposite shows antibacterial activity which comes from the silver nanoparticles mostly. This composite may be applied in many areas such as filter membrane systems removing heavy metals and bacteria from water [118].

Zinc oxide (ZnO) nanoparticles exhibit photocatalytic and antimicrobial properties. It has a great potential in the field of new hybrid materials useful in medicine or environmental protection. For example ZnO was incorporated to the wide range of polymers such as PEO, PVP or PVA. ZnO nanoparticles were also incorporated into the PLA fibers by a combination of electrospinning and electrospraying. This hybrid fibrous material combines the beneficial properties such as biodegradability, photocatalytic and antibacterial properties of the polymer and inorganic filler [112].

Nanoparticles of TiO_2 may be also incorporated into the polymer fibers, for example cellulose acetate electrospun fibers. This composite may contribute to the development of drug delivery systems, material template fabrication or in the field of fibril fillers for composite materials. However at high nanoparticle concentrations aggregation may occur inside the polymer [113].

Iron-platinum (FePt) nanoparticles with 4 nm size were incorporated to PCL fibers This non-woven fiber net provides highly porous microstructure which can be useful in various fields of applications, such as magnetic filtration and drug delivery [119].

In the case of a ferrofluid, colloidal suspension of magnetic particles with magnetic and magneto-optical properties was prepared. This hybrid composite consists of PET nanofibers and aforementioned ferrofluid may be applied such as the sensors or intelligent bulletproof vest [68].

PVA is a promising polymer with wide range of applications due to its properties. PVA is frequently used material in the biomedical research, because of its water-solubility, biocompatibility and hydrophilicity. PVA and carboxy-methyl (CM) chitosan are considered to be promising carriers of silver nanoparticles for biomedical applications. One of the most widely used natural polysaccharides - chitosan and its derivates, are also used in biomedical applications for its biocompatibility and biodegradability. In the case of preparation of PVA/CM-chitosan/AgNPs sample, there are two methods for obtaining nanoparticles with regard to electrospinning process. Heating or microwave irradiation affects on polymer solution with silver ions [120, 121] and reduces nanoparticles. Then the solution is ready for spinning process. Silver nanoparticles may be reduced during the process of fiber preparation fibers also by heating or UV irradiation [122, 123].

In following experiment CM–chitosan and PVA was used as reducing agents and stabilizers. PVA plays a role as a stabilizing agent due to free electrons in oxygen in the -OH group. Moreover, antimicrobial activity of PVA/CM-chitosan/AgNPs samples against *Escherichia coli (E. coli)* was also controlled. Thus PVA/CM-chitosan/AgNPs fibers may be used as potential biomaterial with antibacterial properties [124].

Another experiment examined chitosan/sericin/PVA fibers with incorporated silver nanoparticles. As it was mentioned above, chitosan may be used in many applications such as filtration, drug-delivery, tissue engineering or wound dressings. There are intermolecular interactions between chitosan and sericin as well as between chitosan and PVA through the hydrogen bonding. All of these compounds are responsible for reduction of silver ions to silver nanoparticles. This type of fibers completely inhibited bacterial growth and showed 100 % antibacterial activity against *E. coli* [125].

PVA/AgNPs and PVP/AgNPs fibers were tested against chosen microorganisms such as *E. coli*, *Stahylococcus aureus (S. aureus)* and *Pseudomonas aeruginosa (P. aeruginosa)*. Total growth inhibition after 24 hours was observed. Nanoparticle size ranged between 9 – 11 nm. Nanoparticles were prepared by two methods: for PVA fibers by thermal synthesis and for PVP fibers via chemical reduction of silver nitrate. Moreover, antibacterial testing using disc diffusion test exhibited larger inhibition zone in PVA/AgNPs sample than in PVP/AgNPs sample [126]. Incorporated silver nanoparticles help to scarless healing or improve properties of cosmetic products [127].

PVA can form a mixture with poly(aniline) (PANI). Then silver nitrate ($AgNO_3$) salt was added to the mixture of PVA/PANI. Silver nanoparticles reduced from metal precursor

affected on the electrospinning process during fiber preparation. Smooth fibers with a narrow diameter distribution range (300 – 400 nm) were prepared [128].

PVA/cyclodextrin/$AgNO_3$ mixture was electrospun into PVA/AgNP composite. Cyclodextrin was used as a stabilizing and reducing agent for the silver nanoparticle formation. It was observed that the homogeneous distribution of silver nanoparticles without aggregation was achieved in the electrospun PVA/cyclodextrin fibers. Antibacterial tests for PVA/AgNP and PVA/cyclodextrin/AgNP composite against *E. coli* and *S. aureus* were performed [129].

In conclusion, various types of nanoparticles may be incorporated into the polymer fibers. Nanoparticles contribute to special fiber properties and enable a wide range of utilization especially in the tissue engineering or wound dressings.

3. EXPERIMENTAL PART

3.1 Methods and material

In this thesis part, the main goal is the preparation of biosynthesized silver and gold nanoparticles in the form of powder bionanocomposites and colloidal solutions. These nanoparticles are subsequently incorporated to polymer fibers. Two spinning techniques for polymer fiber formation were used such as centrifugal spinning and electrospinning.

3.1.1 Bionanocomposites and colloids preparation

Diadesmis gallica cells – brown algae - were used in metal nanoparticles biosynthesis. Diatom culture (*Diadesmis gallica* CCALA 766; DG) was obtained from the Culture Collection of the Centre of Algology in Třeboň, Biology Centre of AS CR, Institute of Hydrobiology, Czech Republic. Strains were aseptically cultivated in 1 L Erlenmayer flasks with cotton plugs in WC medium (Guillard and Lorenzen, 1972) with subsequent water glass ($Na_2SiO_3 \cdot 9H_2O$) addition. Diatom strains grew in a special growth chamber (KBN-240, Binder, Germany) with optimal conditions: temperature 24°C in 16 h/8 h light/dark cycle (Figure 7).

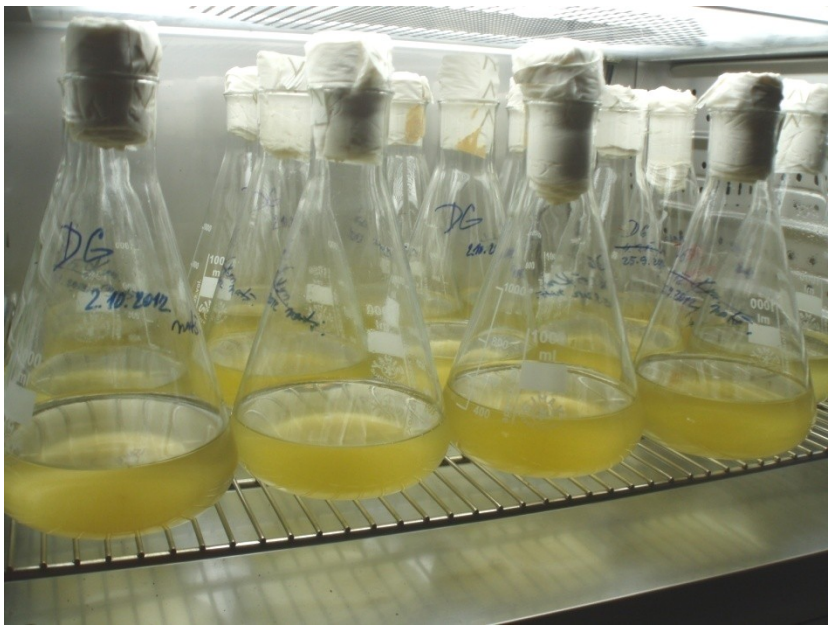

Figure 7: Erlenmayer flasks with diatom cultures in a growth chamber

Algae culture was cultivated approximately 4 weeks to reach a stationary growth phase. During algae growth, the WC medium was decanted and refreshed after every 7 days. In some cases, algae growth was stopped and diatom culture lost their viability. Dead

diatom bodies were also used in biosynthesis experiments to evaluate their ability in nanoparticle synthesis.

Biosynthesis process for living diatom cells consists of a few steps:

- living diatom cultures were decanted into graduated cylinder to obtain an accurate amount of algae biomass;
- the remaining medium obtained from the culture decantation was added to get the ratio 1:20 (diatom culture : medium) - this ratio follows from the optimization of biosynthesis process due to maximum utilization of reducing biomass potential [31];
- after this, an appropriate amount of metallic precursors was added in the ratio 1:1 with regard to the total quantity of diatom culture mixed with medium;
- to form silver nanoparticles, 0,001 M $AgNO_3$ solution was used
- to form mixture of silver and gold nanoparticles, 0,001 M $AgNO_3$ solution and 0,001 M $HAuCl_4$ solution were used

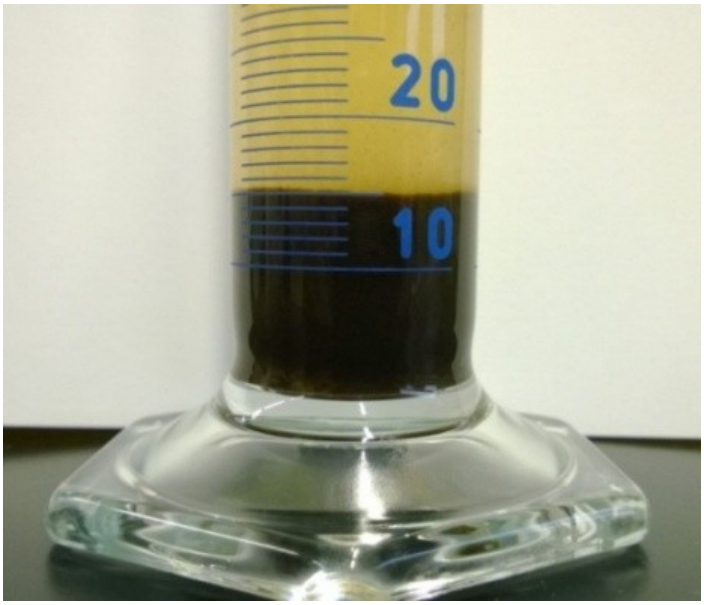

Figure 8: An illustration photo of biomass volume measurement [31]

Suspensions in 200 mL beakers were incubated in the fridge (dark, 5 °C) for 5 days to obtain diatom suspension with synthesized metallic nanoparticles.

Biosynthesis process with dead diatom cells was carried out in the same manner as in the case of living organisms.

After bioreduction every suspension was inserted into a centrifugal apparatus and centrifuged 1 x 6 min at 2000 rpm and 3 x 10 min at 2500 rpm. After first set of

centrifugation, the colloids above the sediment were separated. Next centrifugation cycles served as washing processes using a demineralized water to eliminate the presence of medium and precursor residues.

The term colloid introduced Thomas Graham in 1861 as a suspension of one substance in the second, which even after long periods of standing are separated. Colloids consist of dispersion phase and dispersion medium. They are very fine dispersions containing particles of size from 0.5 to 300 nm [61, 130].

Colloids were subsequently stored in the fridge and sediments (diatom cells with nanoparticles) were dried at 37 °C for 24 hours. A preparation of final samples in colloidal and powder form is presented in a brief sketch (Figure 9).

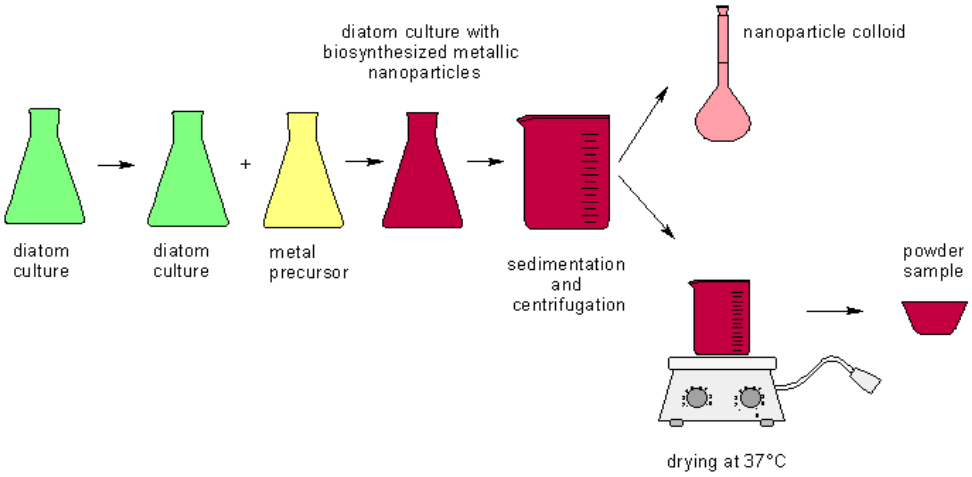

Figure 9: A schematic sketch of colloid and powder sample preparation

3.1.2 Samples designation

In the experiment three types of samples were prepared such as powder bionanocomposites, colloidal solutions of nanoparticles and fibrous PVA samples modified with metallic nanoparticles. Bionanocomposites and colloidal solutions were prepared in two SETs – SET 1 and SET 2. Both SET 1 and SET 2 contain four samples however every SET was prepared in different date. Here, in this chapter a list of prepared samples is included.

Powder samples – bionanocomposites (SET 1 and SET 2):

- DG(L)Ag - diatom composite prepared from living[1] cells with silver nanoparticles
- DG(L)Ag/Au - diatomic composite prepared from living cells containing silver and gold nanoparticles
- DG(D)Ag - diatomic composite prepared from dead[2] diatom cells with silver nanoparticle
- DG(D)Ag/Au - diatomic composite prepared from dead cells with silver and gold nanoparticles

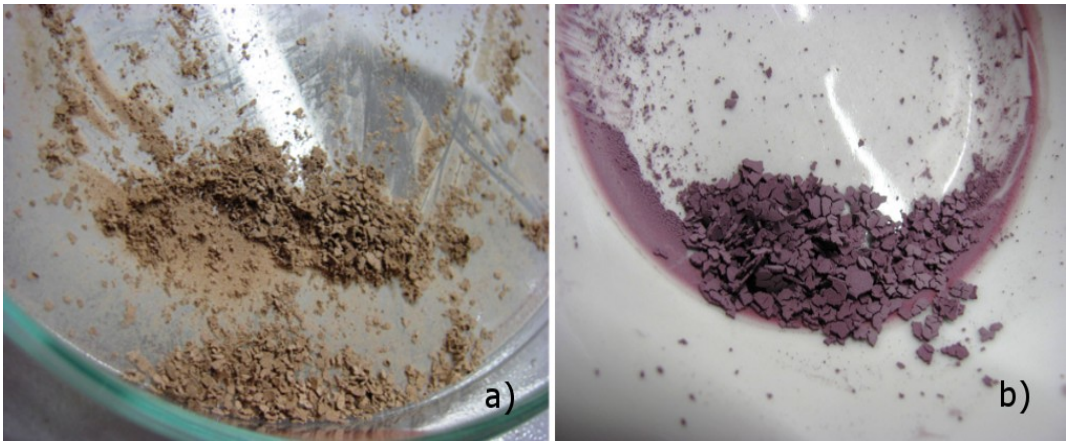

Figure 10: Illustrative photos of a diatomic bionanocomposites: a) DG(D)Ag; b) DG(D)Ag/Au

[1]The term "living cells"means a vital diatom culture before biosynthesis itself.

[2]"Dead cells" are the diatom cultures without visible growth and viability before biosynthesis experiment.

Colloids - colloidal solutions of nanoparticles (SET 1 and SET 2):

- Ag(L) - colloidal solution containing silver nanoparticles prepared using living diatom cells,
- Ag/Au(L) - colloidal solution containing silver and gold nanoparticles prepared using living diatom cells,
- Ag(D) - colloidal solution containing silver nanoparticles prepared using dead diatom cells,
- Ag/Au(D) - colloidal solution containing silver and gold nanoparticles prepared using dead diatom cells.

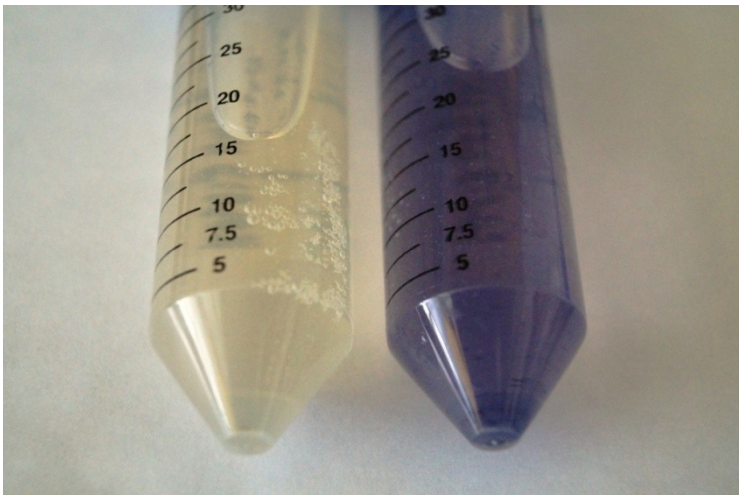

Figure 11: Illustrative photos of nanoparticle solutions; from the left: Ag(L), Ag/Au(L)

3.1.3 Centrifugal spinning method

Each type of spinning requires different parameters and demands for polymer solutions. For purposes of spinning in Pardam (Nové Město na Moravě, Czech Republic), poly(vinyl alcohol) was chosen. In the case of centrifugal spinning, 24 wt% PVA solution was mixed. Because of aqueous character of colloidal solutions PVA was dissolved directly in nanoparticle dispersions. 24 wt % of solid PVA (®Mowiol, M_r = 37 000, Clariant [131]) was dissolved in nanoparticle solution and stirred with magnetic stirrer (speed 200 rpm) for 12 hours at 50 °C. Four types of PVA in nanoparticle solutions were prepared:

1) 24 % PVA +Ag(L),
2) 24 % PVA +Ag/Au(L),
3) 24 % PVA +Ag(D),

4) 24 % PVA +Ag/Au(D).

Centrigufal spinning was carried out on Cyclone L-1000 (Fiberio, USA). 2 ml of a polymer solution was inserted into a rotary spinneret with two attached needles (BD Microbalance 3, 0.3 x 13 mm). PVA/NPs fiber was formed on metal collectors arranged in a circle. Distance between rotation center of a spinneret and collector was 18 cm.

One spinning cycle took 10 minutes. Few spinning cycles were performed to obtain an appropriate amount of PVA/NPs fibers. Spinning speed was also controlled and optimized between 4500-7000 rp. All experiments occurred at working temperature 20 °C with 50 % humidity of the air.

Figure 12: Cyclone L-1000 machine used in centrifugal spinning method (Fiberio) [132]

3.1.4 Electrostatic spinning process using Nanospider machine

Electrostatic fiber formation was performed on Nanospider NS 1WS500U (Elmarco, Czech Republic) in Department of Nonwovens and Nanofibrous materials, Technical University of Liberec (Czech Republic) (see Figure 13). Sloviol (16 % wt solution of PVA) was diluted to 10 wt % concentration with nanoparticle colloidal solution. In addition, samples containing powder bionanocomposites were also prepared as follows: to 10 wt % solution of PVA (clear PVA solution prepared with distilled water) an optimal weight of DG(L)Ag or DG(L)Ag/Au was added to obtain 12.6 % wt in PVA fibers. Suspensions were sonicated for 1 min to reach a homogeneous structure. Six fibrous samples were prepared:

1) 10 % PVA +Ag(L),
2) 10 % PVA +Ag/Au(L),
3) 10 % PVA +Ag(D),
4) 10 % PVA +Ag/Au(D),

5) 10 % PVA + DG(L)Ag,
6) 10 % PVA + DG(L)Ag/Au.

Because of noticeable influence of water surface tension, an optimum amount of ethanol was added to decrease this negative effect [133]. An appropriate amount of the polymer (about 20 g) was inserted into the spinning unit. According to Nanospider product profile spinning cycle runs approximately 60 min per batch [134]. The charge for electrode 60 kV was positive and collector 15 kV was negative; distance between collector and electrode was 21 cm. PVA/NPs fibers were formed on a spunbond. The experiment occurred at working temperature 23.2 °C with 23 % humidity of the air.

Figure 13: Photographs of Nanospider™ machine for electrostatic spinning method and supplementary equipment; from the left: Nanospider™ NS 1WS500U, data processing equipment and spunbond textile for fiber collection [134]

3.1.5 Bionanocomposites, nanoparticle suspension and fibrous samples characterization

3.1.5.1 Transmission Electron Microscopy (TEM)

Gold and silver nanoparticles were characterized by transmission electron microscope FEI Morgagni with standard tungsten filament and side-entry CCD camera MegaView III and iTEM imaging software at Institute of Cellular Biology and Pathology, Charles University in Prague (Czech Republic). Samples were resuspended in ethanol and applied on carbon/formvar coated mesh copper grids.

Powder samples, nanoparticle suspensions and fibrous samples were also characterized by transmission electron microscope JEOL 1200 EX at Institute of Electrical Engineering, Slovak Academy of Sciences in Bratislava (Slovak Republic). Powder samples were stirred in distilled water, then an appropriate amount of a specimen was put on a carbon grid.

3.1.5.2 Nanoparticle size distribution

Size distribution of biosynthesized nanoparticles in powder bionanocomposites was performed by JMicroVision program (image analysis). At least 300 nanoparticles from TEM micrographs underwent the image analysis per sample. All calculations and histograms were created by MATLAB software.

Obtained data from image analysis were processed by statistics in which a number of particles is in a certain size class. From measured data statistic quantities were calculated: probability density, arithmetic mean, standard deviation and modus. Formulas were adjusted based on the literature [135].

1. probability density

$$q_0(x_i) = \frac{n_i}{\Sigma n_i}$$

2. arithmetic mean

$$\bar{x}_A = \frac{\Sigma(x_i \cdot n_i)}{\Sigma n_i}$$

3. standard deviation

$$\sigma = \sqrt{\frac{\Sigma q_0(x_i) \cdot (x_i - \bar{x}_A)^2}{N-1}}$$

4. modus = shows the most represented value in the distribution [135]

Size distribution of nanoparticles in colloidal solutions was determined by CPS Disc Centrifuge DC – 240 000 in Bulk Laboratory in VŠB - Technical University of Ostrava (Czech Republic). This centrifugal granulometer is designed for measuring particles in the range from 0.01 micrometers to 40 micrometers, with the greatest effectiveness achieved from 0.02 microns to 30 microns.

3.1.5.3 Scanning Electron Microscopy (SEM)

Fibrous samples were characterized by scanning electron microscope FEI Quantum FEG 450 at Regional materials science and technology centre in VŠB - Technical University of Ostrava (Czech Republic). A Secondary Electron Detector (SED) and Back-Scattered Electron Detector (BSED) were used.

3.1.5.4 X-RAY diffraction (XRD)

The XRD patterns were recorded under Co Kα irradiation (λ = 1.789 Å) using the Bruker D8 Advance diffractometer (Bruker AXS) equipped with a fast position sensitive detector VÅNTEC 1. Measurements were carried out in the reflection mode, powder samples were pressed in a rotational holder, goniometer with the Bragg-Brentano geometry in 2 θ range from 3 to 75, step size 0.03° was used. Phase composition was evaluated using database PDF 2 Release 2004 (International Centre for Diffraction Data). Measurements were performed in Nanotechnology Centre, VŠB - Technical University of Ostrava.

XRD analysis was also carried out using Bruker D8 DISCOVER diffractometer (Bruker AXS) equipped with X - ray tube with rotating Cu anode (λ = 1.5418 Å) operating at 12 kW. All measurements were performed in parallel beam geometry with parabolic Goebel mirror in the primary beam. The samples were prepared in the form of thin layers of powder fixed to a glass plate. The X - ray diffraction patterns were recorded in grazing incidence set-up in the angular range 2θ from 20° to 80° with the step size 0.05° and with the angle of incidence α = 1.5°. The advantage of this method is that the measured intensities as well as the precise position of the diffraction maxima are insensitive to the surface irregularities/roughness. Measurements were performed at Institute of Electrical Engineering, Slovak Academy of Sciences in Bratislava (Slovak Republic).

3.1.5.5 Elemental analysis using Inductively Coupled Plasma Atomic Emission Spectroscopy

An elemental analysis was performed on ICP - AES (Inductively Coupled Plasma Atomic Emission Spectroscopy) spectrometer Ciros Vision (SPECTRO Analytical Instruments Inc., Germany). Colloids were filtrated through a fine filter paper and then aliquots were boiled with aqua regia. In the case of solid samples first the silica matrix of diatom was dissolved using hydrofluoric acid. Subsequently samples were mixed with aqua regia. All analysis was performed in Nanotechnology Centre, VŠB - Technical University of Ostrava.

3.1.5.6 Fourier Transform Infrared Spectroscopy (FTIR)

FTIR spectrometer Nicolet 6700 FT-IR spectrometer (Thermo Nicolet, USA) is a variable spectroscopic system for many applications. The interferometer Vectra achieved standard nominal spectral resolution 0.4 cm^{-1}. FTIR spectrometer works by ATR using an

ATR diamond head. The operating unit is fully automatic and takes place via computer software Omnic.

The spectra were measured in the range of 400 – 4 000 cm^{-1}. Spectra were arranged using the ATR correction with automatically modified baseline. A presence of CO_2 bands was removed. FTIR analysis was performed in Nanotechnology Centre, VŠB - Technical University of Ostrava.

3.1.6 Antibacterial activity evaluation

Antibacterial activity of powder bionanocomposites was tested. Bacteria cultures *Bacilus cereus* CCM 868 ($6.3 \cdot 10^8$ CFU/ml), *Staphylococcus aureus* CCM 299 ($3.5 \cdot 10^9$ CFU/ml), *Streptococcus agalactiae* CCM 6187 ($2.1 \cdot 10^9$ CFU/ml), *Escherichia coli* CCM 3954 ($9.4 \cdot 10^8$ CFU/ml) and *Pseudomonas aeruginosa* CCM 1960 ($5.1 \cdot 10^8$ CFU/ml) were obtained from Czech Collection of Microorganisms (Brno, Czech Republic). They were cultivated onto the agar plate at 37 °C.

Minimum inhibition concentration (MIC) is determined by the lowest concentration of an antimicrobial agent that will inhibit the visible growth of a microorganism after overnight incubation of bacteria cells [136]. Samples in the growth media were diluted to achieve the following concentrations: 1.12 % wt., 3.3 % wt. and 10 % wt. of DG(L)Ag, DG(L)Ag/Au sample (or DG(D)Ag, DG(D)Ag/Au respectively). The preparation of the suspensions and the evaluation of the bionanocomposite antibacterial activity were carried out as follows:

- 0.05 g of powder sample were weighed out into the Eppendorf flasks,
- 450 μL of PBS (phosphate buffer saline) was subsequently added to create 10 %. wt. of bionanocomposite,
- to prepare the solutions with 3.3 % wt. 167 μL from the previous solution was taken to eppendorf flasks with 330 μL of PBS,
- for preparation of solutions with 1.12 % wt. 167 μL from the previous solution was taken to eppendorf flasks with 330 μL of PBS,
- 100 μL of bacterial cultures were added to all samples,
- part of the solutions with cultures of bacteria was left in stationary position in laboratory conditions (23°C, moderate light) for 24 hours, remaining part of solutions was agitated in horizontal shaker with shaking speed of 400 rpm in laboratory conditions (23°C, moderate light) for 24 hours,

- after 24 hours solutions were applied onto agar plates and subsequently incubated at 37°C,
- samples were observed after 24, 48 and 72 hours.

Fibrous samples 10 % PVA + DG(L)Ag and 10 % PVA + DG(L)Ag/Au were assessed by a disc diffusion test. Bacteria cultures *Staphylococcus aureus* CCM 4223, *E. coli* CCM 4225 and *Pseudomonas aeruginosa* CCM 3955 were obtained from Czech Collection of Microorganisms (Brno, Czech Republic).

Into the glucose broth medium selected bacterial cultures were put and the final suspension was diluted with water to 0.5 McFarland units. Suspension turbidity was measured by DEN - 1 McFarland Densitometer (BioSan). Suspension was put onto a Petri dish with Müller - Hinton agar and excessive amount was poured away. Then the fibrous samples were put and incubated at 37 °C for 24 hours (in biological thermostat BT 120).

4. RESULTS AND DISCUSSION

4.1 Study of sample morphology and nanoparticle size distribution

TEM analysis confirmed a presence of metallic nanoparticles in powder bionanocomposites as well as in the colloids. First of all, bionanocomposites will be discussed.

First picture (Figure 14a) shows diatom bodies with synthesized metallic nanoparticles. Nanoparticles on the surface of diatom are not well dispersed as well as it is seen on Figure 14b. Nanoparticles are often located in the diatom biological matrix where they are stabilized. Nanoparticles gained mostly spherical shapes in every type of powder bionanocomposite. An average size of silver nanoparticles was approximately **17 nm** for DG(L)Ag and **22 nm** in DG(D)Ag. The highest proportional representation (modus) of silver nanoparticles was between **9 - 12** nm in DG(L)Ag and **6 - 9** nm in DG(D)Ag as it is seen in graphs (Figure 15, Figure 16).

According to previous results [30-32] the size distribution was reduced because of synthesis at 5 °C. Higher temperature may cause synthesis of bigger nanoparticles.

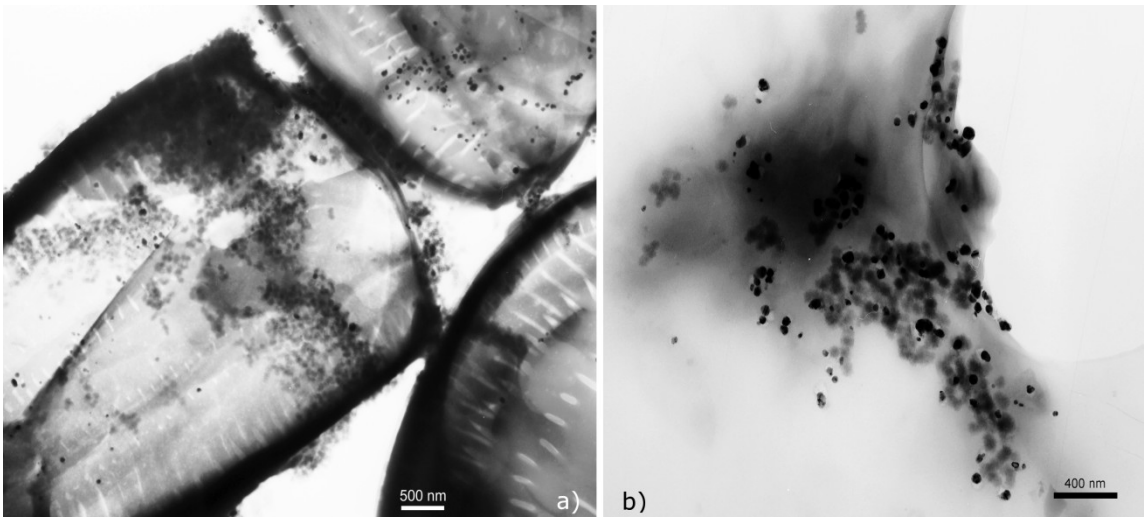

Figure 14: TEM micrographs of silver nanoparticles in DG(L)Ag powder sample, SET 2

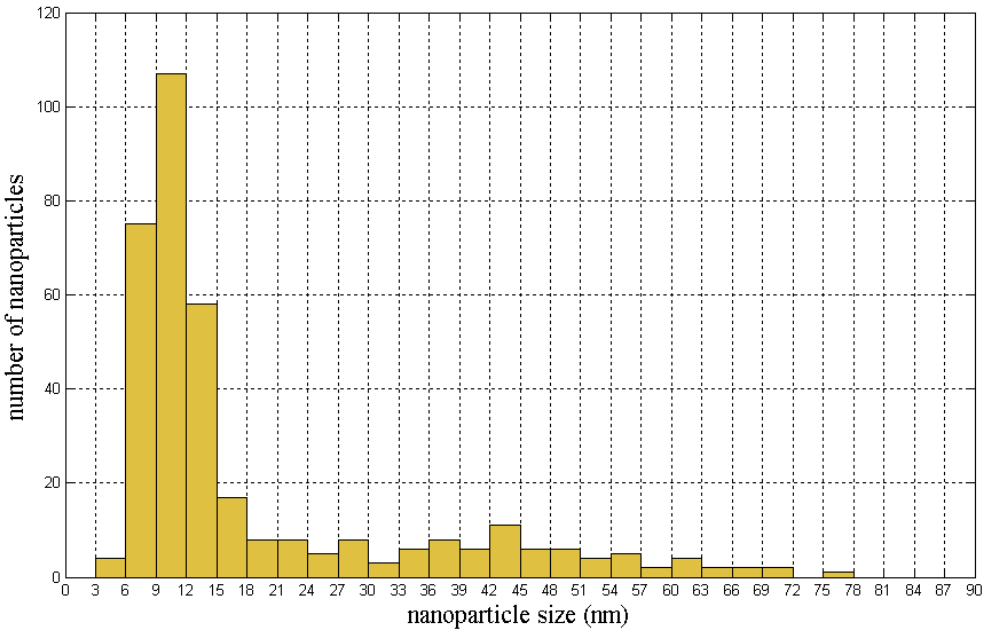

Figure 15: Histogram of size distribution of silver nanoparticles in DG(L)Ag sample

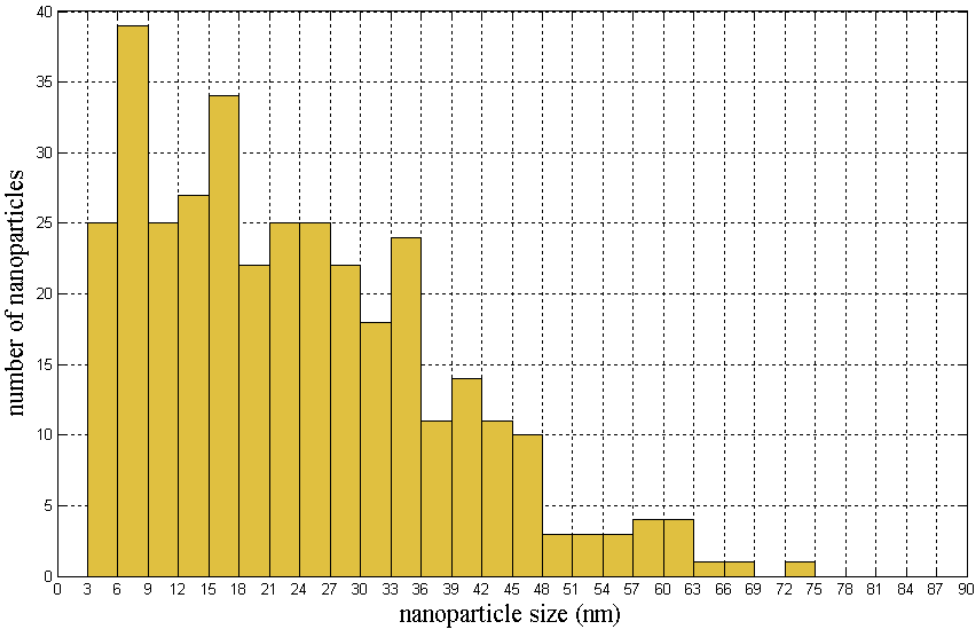

Figure 16: Histogram of size distribution of silver nanoparticles in DG(D)Ag sample

Silver and gold nanoparticles in powder sample DG(D)Ag/Au are documented on the Figure 17. In these types of samples with combination of metals there is no possibility to distinguish what type of metal the nanoparticle is. However, according to TEM images and image analysis the size of metallic nanoparticles in the DG(L)Ag/Au sample is approximately **20 nm**.

In the case of DG(D)Ag/Au nanoparticles were much smaller and sizes were approximately **8 nm**.

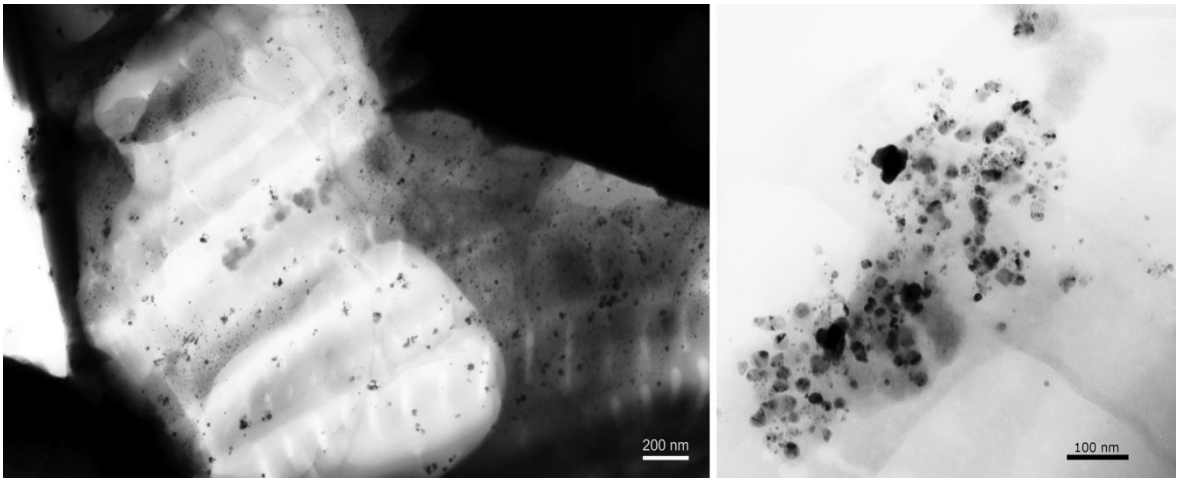

Figure 17: TEM micrographs of both silver and gold nanoparticles in DG (D)Ag/Au powder sample (SET 2)

Size distribution of powder samples with both silver and gold nanoparticles is shown on Figure 18 and Figure 19.

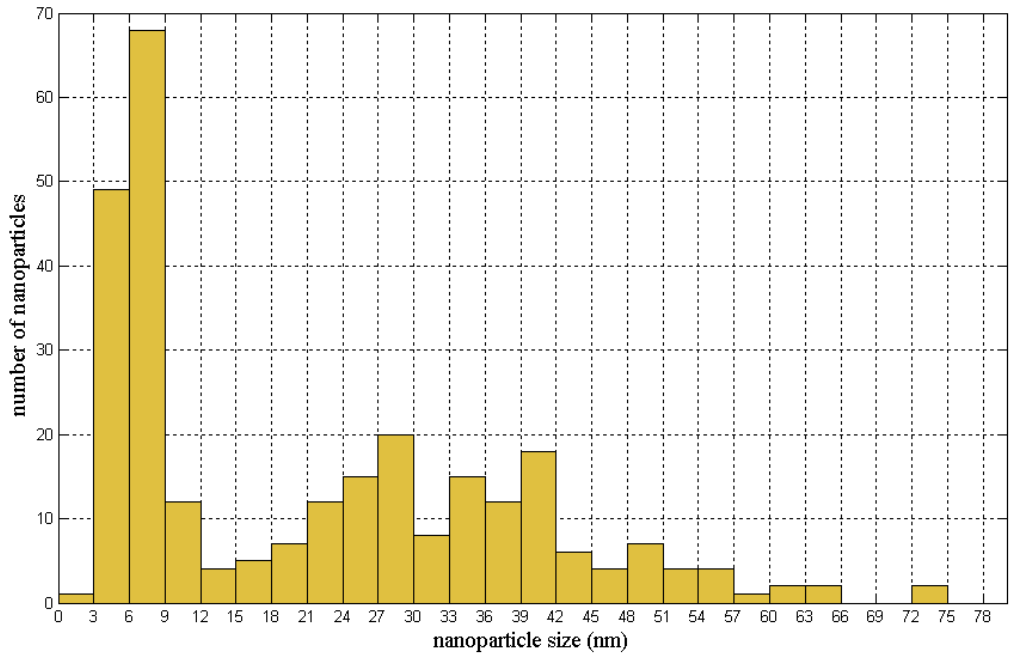

Figure 18: Histogram of size distribution of metal nanoparticles in DG(L)Ag/Au

The highest proportional representation of nanoparticles in DG(L)Ag/Au sample was between **6 - 9 nm** and, surprisingly, the same trend was in DG(D)Ag/Au sample. But the size distribution in the case of bionanocomposite from living cells was wider than in the

case of a dead cells sample. In DG(D)Ag/Au the size distribution of nanoparticles was narrower and nanoparticles bigger than 33 nm were not present.

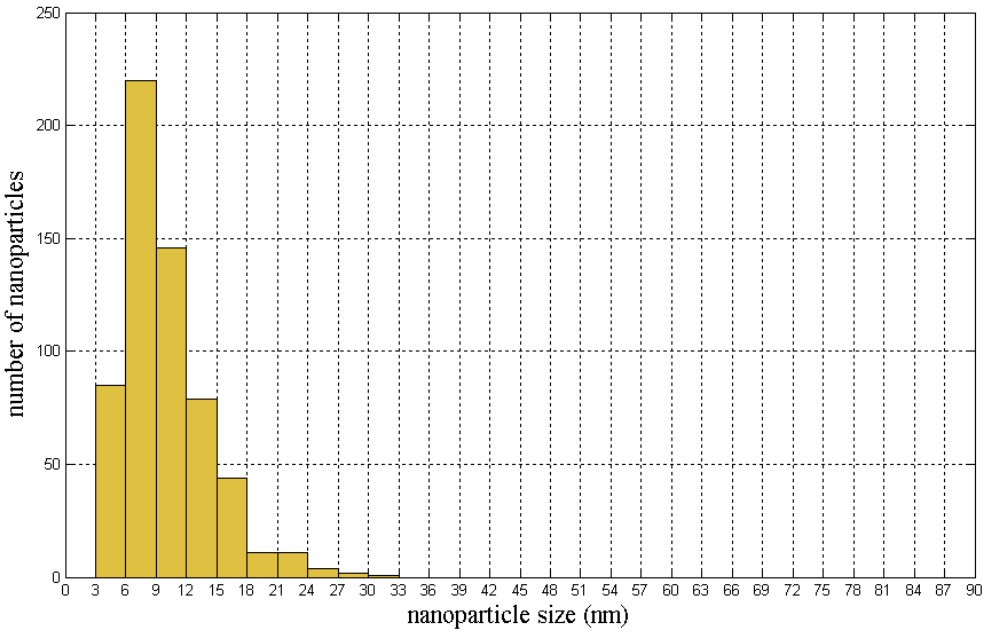

Figure 19: Histogram of size distribution of metal nanoparticles in DG(D)Ag/Au

Table 3 summarizes an arithmetic means and corresponding standard deviations. All calculated values used in statistics are shown in Appendix.

Table 3: Summary of arithmetic means of metallic nanoparticles in powder bionanocomposites

Sample	Arithmetic mean (nm)	Standard deviation (nm)
DG(L)Ag	17.187	± 0.812
DG(L)Ag/Au	20.029	± 0.998
DG(D)Ag	22.151	± 0.768
DG(D)Ag/Au	8.316	± 0.176

The particle size of the colloidal solutions was measured by CPS Disc Centrifuge. Unlike nanoparticles deposited on diatom silica frustules, particles in the solutions disposed of larger sizes and wider size distribution. First, as it is seen on TEM images (Figure 20, Figure 21) the nanoparticles in colloids were coated with some organic components leading to formation of clusters. Clusters consisted of the nanoparticles stabilized with organic matter, thus cluster did not contain nanoparticles aggregates. These clusters were dispersed in colloidal solutions and probably released during centrifugation

process. Clusters were not considered as nanoparticle aggregates, but as larger slime pieces of organic origin serving as a stabilizer, which came from the diatom metabolism.

The particle size was measured relative to the particle weight. The weight of all particles in the sample was determined in a particle size measuring unit then the size relative to the mass fraction was assessed. Particle size measuring unit detected nanoparticle size distribution increased by the size of surrounding organic stabilizers. Despite this fact, the size distribution generally agrees with the TEM images.

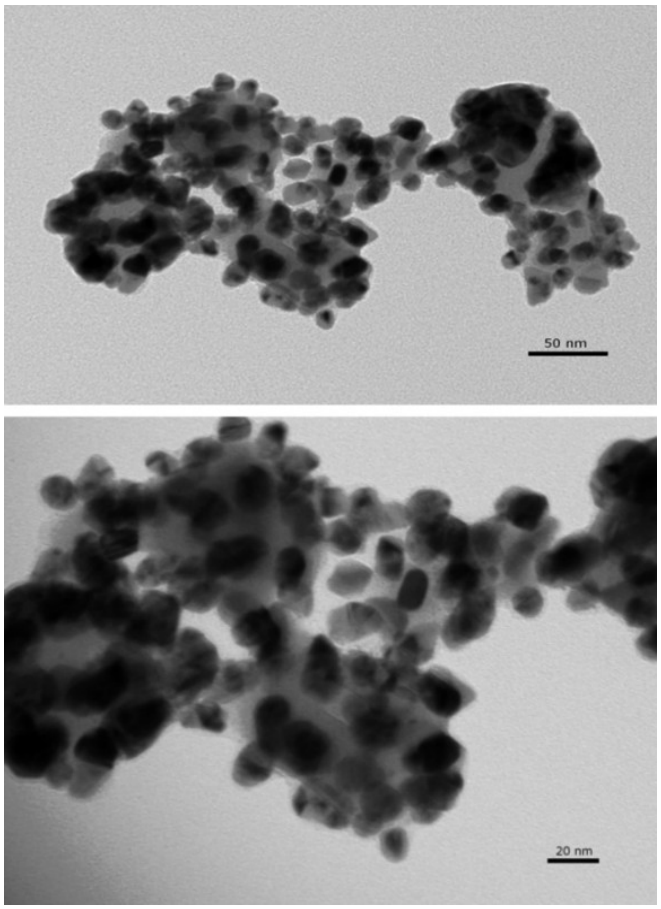

Figure 20: TEM micrographs of Ag/Au(L) nanoparticles solutions (SET 1)

Each sample was measured only once. Therefore, standard deviation disposed of high values. Given the small amount of Ag/Au(D) solution it was not possible to determine the size distribution. According to the assumption this sample may show similar character as the rest measured samples.

Average size value of Ag nanoparticles in the Ag(L) colloid was determined to **47.5 nm**, however particles showed the largest distribution in the range from 50 to 63.1 nm. Size distribution in this sample was broad, even though nanoparticles of sizes smaller than 50 nm were also represented.

The largest particle mean size was found for Ag/Au(L) sample. Although the largest size distribution was between 50 to 63 nm, mean size value was determined to **63 nm**. In Ag/Au(L) sample, nanoparticles larger than 50 nm could be observed as well. This may represent a frequent occurence of organic residues in which the nanoparticles were stabilized. In the case of Ag(D) sample the average nanoparticle size was **39 nm**, modus values were shown between 31-39.9 nm. A summary of size means is shown in Table 4, all distribution values based on CPS Disc Centrifuge data are mentioned in Appendix.

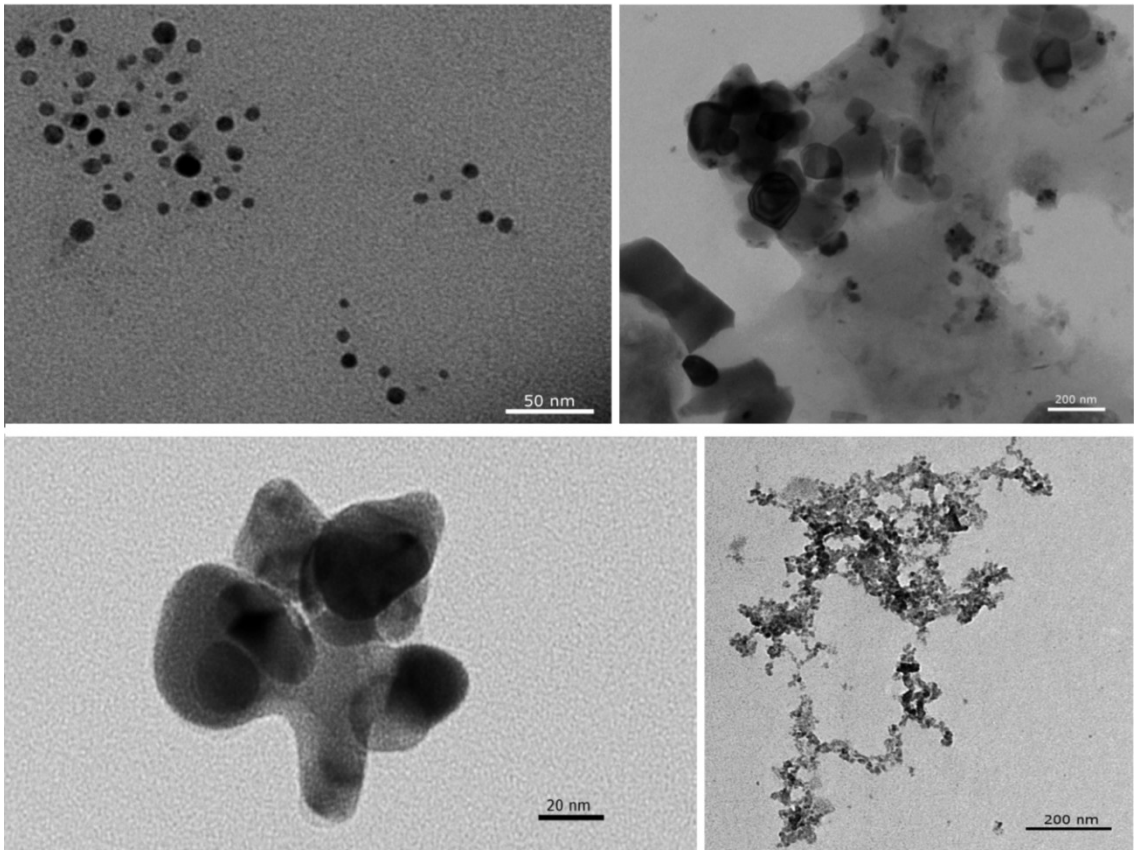

Figure 21: TEM micrographs of nanoparticle solutions: two upper pictures are Ag(D) colloids (SET 1); two bottom photos show Ag(L) samples (SET 1)

Nanoparticles in colloidal solutions as well as attached on diatom frustules may be synthesized in different shapes (Figure 22). Mostly spherical shapes of silver and gold nanoparticles were observed. Moreover, triangular or square shaped nanoparticles were also noticed.

Table 4: Summary of arithmetic means of metallic nanoparticles in colloids

Sample	Arithmetic mean (nm)	Standard deviation (nm)
Ag(L)	48.400	± 14.600
Ag/Au(L)	49.400	± 17.000
Ag(D)	41.800	± 13.800
Ag/Au(D),	57.700	± 14.700

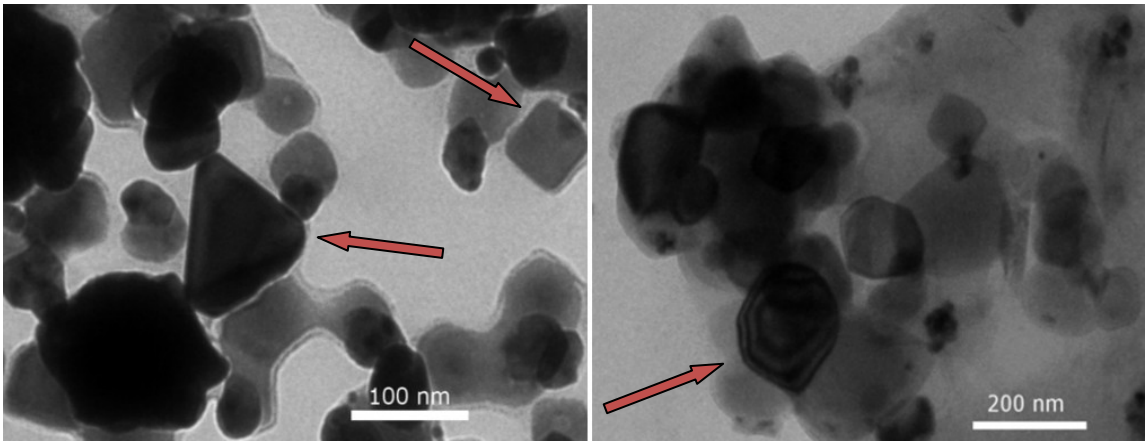

Figure 22: TEM micrographs of variable shapes of silver or gold nanoparticles

4.2 Study of powder samples crystallography

Two sets (SET 1, SET 2) were analyzed using X-Ray diffraction to confirm presence of metals primarily. Both sets exhibited a similar character. In all samples from the SET 2 (Figure 23), a presence of cubic silver (Ag) was confirmed. The most significant peak characterizing cubic silver was in DG(L)Ag and DG(D)Ag sample. Peaks characterizing Ag in a the cubic form were not noticeable in other two diffractograms of DG(L)Ag/Au and DG(D)Ag/Au sample because of their lower intensities.

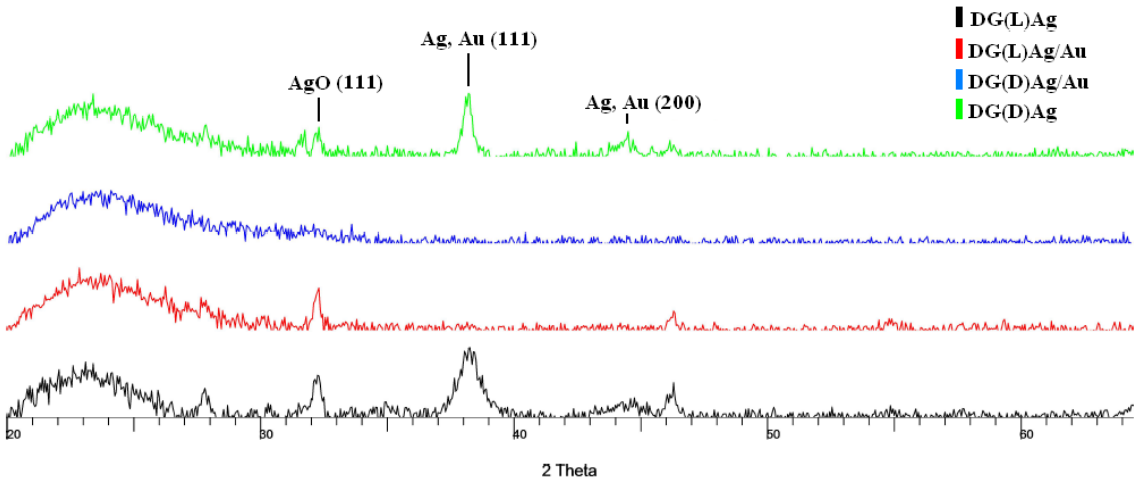

Figure 23: Diffractograms of powder bionanocomposites (SET 2)

Moreover, silver can be found in its oxidized form (AgO). This phenomenon can be explained by the fact that part of the silver nanoparticles was oxidized and part remained in crystalline form. This corresponds with the general assumption that silver is sensitive to the presence of oxygen and may be easily oxidized [137]. Silver oxide was present in all samples and the peak was found around 32° of 2θ angle [138, 139]. On the other hand oxidized forms of gold were not found, because gold exhibits a higher stability [140].

In the case of samples with both silver and gold (Au) nanoparticles it was not possible to distinguish peaks. A peak for silver and gold overlapped around 38° of 2θ angle and at 44° of 2θ value therefore there was one single peak for cubic silver and cubic gold. It was valid for (111) plain as well as for (200) plane. Measured data are in agreement with previous research and scientific articles [37, 41, 42, 141-145].

The region between 20° and 30° of 2θ angle described an amorphous nature of measured bionanocomposites. These diffraction lines showed the presence of silica which

corresponds to the silica frustules of diatoms. The samples had a slight crystalline character and did not contain many crystal domains in which diffraction could occur.

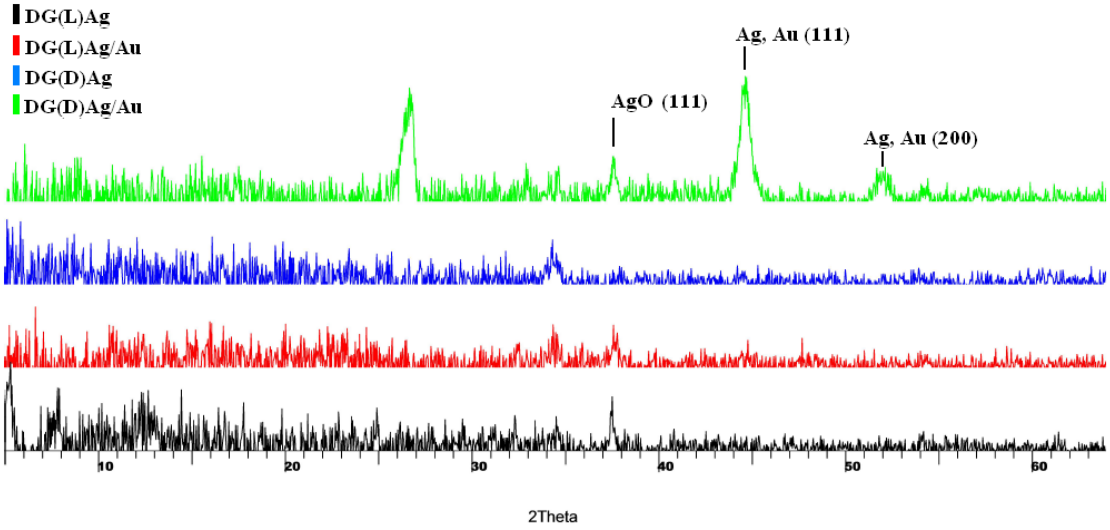

Figure 24: Diffractograms of powder bionanocomposites (SET 1)

Powder samples from SET 1 were analyzed (Figure 24). As was mentioned above the similar characters in both SETs were noticed. There was no difference in the term of peak intensities of measured metals.

Unlike of sample from SET 2 these samples disposed of a visible peak characterizing Ag and/or Au. Diffraction lines had apparent maximums in aforementioned 2θ values for silver and gold. As was seen in SET 2 sample silver was also present in oxidized form Ag_2O. Every sample containing silver or both silver and gold included silver oxide. As well as in previous samples, an amorphous region in diffractogram was noticed. A one sharp peak in the region of 20° and 30° of 2θ angle appertained to silica (SiO_2) origin as was mentioned in previous spectra. A presence of diatomic structures was evident in all samples.

4.3 Elemental analysis of silver and gold amount in the samples

ICP-AES method is suitable for detection of metal content in the samples. An elemental analysis of powder bionanocomposites confirmed the presence of metallic nanoparticles in specific amounts.

Two sets (SET 1, SET 2) of powder bionanocomposites were assessed. The SET contained four samples (prepared using biosynthesis, but in different date):

1) DG(L)Ag,
2) DG(L)Ag/Au,
3) DG(D)Ag,
4) DG(D)Ag/Au.

Because of the dynamic nature of processes during biosynthesis the same amount of metallic nanoparticles (Ag or Ag/Au) was not obtained even though the biosynthesis was optimized. According to the assumption biosynthesis with dead cells may be performed in different manner than biosynthesis with living cells. Thus, a final nanoparticle quantity may be also different and ICP-AES analysis confirmed this.

The living biomass may dispose of greater number of functional reducing groups, thus it may have a higher reducing potential. Nevertheless, according to the ICP-AES data the reducing potential of living cells may be closely similar to the dead biomass. An amount of metals in both types of composites was similar or lower as it is seen in DG(L)Ag or DG(D)Ag (Table 5) samples.

Table 5: A summary of metal contents in powder bionanocomposites

Analyte	Ag [wt %]	Au [wt %]	Ag [wt %]	Au [wt %]
	SET 1		SET 2	
Sample				
DG(L)Ag	0.76 ± 0.08	-	0.39 ± 0.04	-
DG(L)Ag/Au	0.23 ± 0.03	0.89 ± 0.09	0.40 ± 0.04	1.40 ± 0,14
DG(D)Ag	1.01 ± 0.11	-	0.43 ± 0.04	-
DG(D)Ag/Au	0.64 ± 0.07	2.21 ± 0.23	0.46 ± 0.05	1.79 ± 0.18

In samples with combination of both silver and gold a decreasing trend of silver amount was discovered. DG(L)Ag/Au and DG(D)Ag/Au samples contained in the average of three and half times more gold amount comparing with silver amount. An explanation of lower amount of silver in DG(L)Ag, DG(D)Ag may be closely linked with their preparation. As was mentioned in previous chapter during preparation of powder bionanocomposites a centrifugation was performed. Centrifugation process provided a solution with metallic nanoparticles inside. According to a molecular weight of silver (M = 107.87 g/mol [146]) and gold (M = 196.97 g/mol [146]) the silver may be easily released to the solution during centrifugation process. It can be a reason why silver is in minority part in the Ag/Au powder bionanocomposites because of its lower molecular weight. In addition DG(L)Ag and DG(D)Ag had a different nature (unlike DG(L)Ag/Au and DG(D)Ag/Au) during drying a subsequent scrapping off a ceramic bowl, hence a gentle manipulation with the samples was required.

The concentration of Ag and Au in colloidal solutions was measured (Table 6). Four types of nanoparticles solutions were analyzed in two sets as well as powder bionanocomposites.

Table 6: A summary of metal contents in colloidal solutions

Analyte	Ag (mg/L)	Au (mg/L)	Ag (mg/L)	Au (mg/L)
	SET 1		SET 2	
Sample				
Ag(L)	11.300 ± 1.200	-	9.700 ± 1.000	-
Ag/Au(L)	0.330 ± 0.030	2.460 ± 0.250	0.230 ± 0.030	5.260 ± 0.530
Ag(D)	2.820 ± 0.290	-	3.170 ± 0.320	-
Ag/Au(D)	0.033 ± 0.004	0.180 ± 0.020	< 0.050	0.250 ± 0.030

In every SET, similar trends occured. Ag(L) contained the highest amount of silver. The amount of silver in Ag(D) was lower than in Ag(L) and the lowest values of silver amount were found in Ag/Au (D). As in the case of powder bionanocomposites Ag/Au(L) and Ag/Au(D) contained a higher amount of gold than silver. It was important to get ICP-AES data for antibacterial evaluation of bionanocomposites and colloidal solutions in polymer fibers modified with metal nanoparticles.

4.4 Spectroscopic measurement

FTIR spectroscopy was carried out to analyze powder bionanocomposites and PVA fibrous materials. Most functional groups had characteristic absorption bands that did not change from one compound to another [57, 147]. First, the FTIR spectra of the bionanocomposites were described, spectra of modified PVA membranes will follow. During FTIR assessment four types of bionanocomposites were analyzed (see Figure 24):

1) DG(L)Ag,
2) DG(L)Ag/Au,
3) DG(D)Ag,
4) DG(D)Ag/Au.

FTIR analysis confirmed a presence of basic functional groups possibly responsible for biosynthesis [46] as was previously referred for this type of bionanocomposite [31]. In the samples containing silver nanoparticles a strong, broad bands at 3287 cm^{-1} and 1648 cm^{-1} were found (Figure 25). These two bands indicated a presence of OH groups. The region of 4000 to 2500 cm^{-1} among others corresponds to absorptions caused by single-bond stretching motions (O-H bond) [57]. Deformation vibrations of OH groups can be found in lower wavenumbers. The presence of a hydroxyl groups may be a consequence of an inappropriate drying of bionanocomposite or the presence of air humidity.

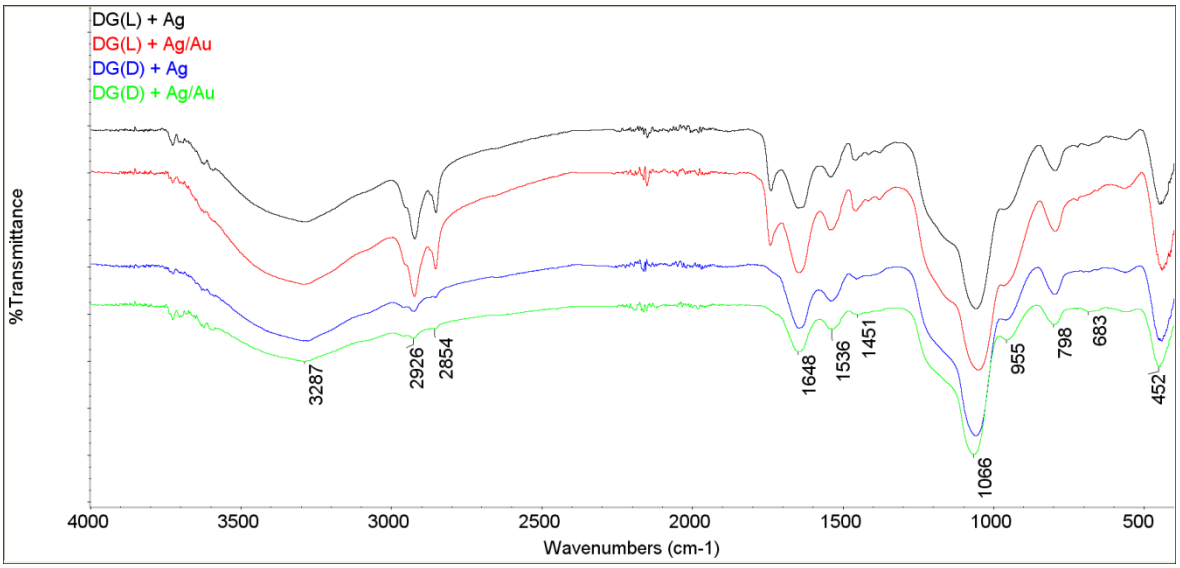

Figure 25: FTIR spectra describing powder bionanocomposites

Bands at positions 2926 and 2854 cm^{-1} can be assigned to C-H of CH_2 groups [148]. Deformation vibrations of these groups were also showed in the region of lower wavenumbers (around 1540 and 1400 cm^{-1}). The presence of CH_2 groups was closely

linked with organic components and compounds in diatoms. In DG(L)Ag sample (prepared from living biomass) a higher intensity of the bands corresponding to CH_2 group was found. It was caused by vital behavior of biomass before biosynthesis. Logically DG(D)Ag samples contain a lower amount of living matter. Therefore CH_2 group had a lower intensity.

On the left side of CH_2 bands (2959 and 2872 cm^{-1}) small bands or a shoulder could be seen which could be linked with CH_3 functional group. This functional group was represented as a minority part in comparison with the CH_2 groups, because of the almost undetectable intensity of the groups in the non-living diatoms.

Because of silica nature, diatom bionanocomposites bands were also found in FTIR spectra. Si-O-Si bonds were presented at 1058 cm^{-1} and Si-O bond at 961 cm^{-1}. Bonds seen in lower wavenumbers were closely linked to silica compounds [31].

The presence of organic compounds arising from living or non-living organisms was clearly showed by band at 1739 cm^{-1} which corresponds to double bond region (C=O) [148]. In the case of samples prepared from living biomass the band was visible and may came from carboxylic acids, esters, aldehydes or ketones [57]. However, in DG(D)Ag the discussed band was not present. Spectroscopic data (FTIR spectra) of DG(L)Ag/Au and DG(D)Ag/Au were significantly similar to previous samples with little differences in DG(L)Ag/Au sample. In DG(L)Ag/Au spectra the band at 1050 cm^{-1} was present. This band was associated with Si-O-Si bond but was shifted towards lower wavenumbers, in comparison with bionanocomposites which contained only silver. Also, a shift towards lower wavenumbers is possibly influenced by the combination of both silver and gold.

FTIR is also a very useful analytical method for evaluation of polymers [149-151] or polymer fibers [125, 147]. Four types of PVA/NPs polymer fibers with nanoparticles were prepared by centrifugal and electrostatic spinning. These samples are shown on Figure 26.

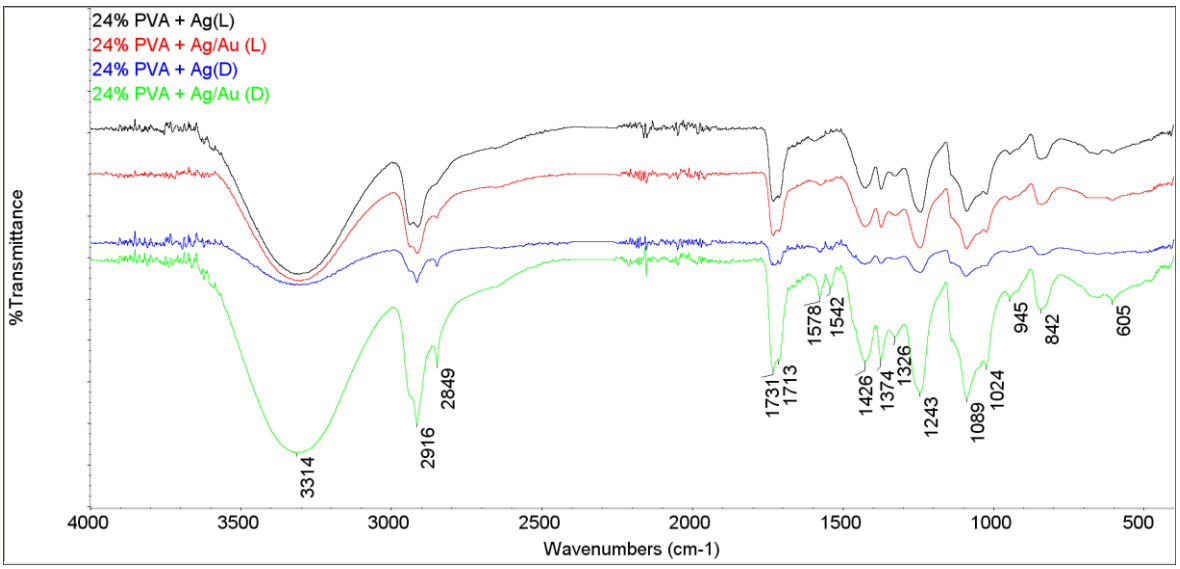

Figure 26: FTIR spectra of PVA fibers prepared with centrifugal spinning

First 24 % PVA + Ag(L) sample wa described. Hydroxyl groups could be seen at 3305 cm^{-1}. As well as in powder bionanocomposites hydroxyl groups may came from water molecule. This is in agreement with scientific research of PVA materials [125, 147, 152]. Furthermore, the presence of OH bonds was also indicated at 1426 cm^{-1} (a deformation vibration). Bands at wavenumbers 1373 and 1325 cm^{-1} [149, 150] were also related with hydroxyl groups.

Bands located at 2939 and 2912 cm^{-1} appertained to C-H bonds in the CH_2 groups whose origin may be from PVA. In addition, deformation vibrations of this group were found at 836 and near 918 cm^{-1} as a shoulder. Because of biological nature of synthesized silver nanoparticles some similar trends with diatomic samples were obtained. For example band at 1731 cm^{-1} corresponded to C=O groups and/or band lying at 1596 cm^{-1} originated from aforementioned diatomic nature. This presumption was confirmed by bands at 1024 and 945 cm^{-1} which appeared because of Si presence. The residues of silica may come from parts of diatom bodies which possibly originated from centrifugation process.

The part of spectra around 1140 $cm^{-1}$was very important, because these shoulders were typical for PVA fibrous structure [147]. In the current sample other bands showed the presence of various bonds as C-C (1089 cm^{-1}), C-O-C (1241 cm^{-1}) or a deformation vibration of C-H (1426 cm^{-1}). Other fibrous samples showed similar trends in FTIR spectra as in the case of 24 % PVA + Ag(L). FTIR spectra also confirmed fibrous structure in all observed samples.

On the Figure 27 FTIR spectra of samples mentioned below were shown:

1) 10% PVA +Ag(L),
2) 10 % PVA + Ag/Au(L),
3) 10 % PVA +Ag(D)
4) 10 % PVA +Ag/Au(D).

Because of the same utilization of nanoparticles solutions and type of polymer, spectra were practically identical with previous results. The most important shoulder around 1140 cm^{-1} showed fiber origin.

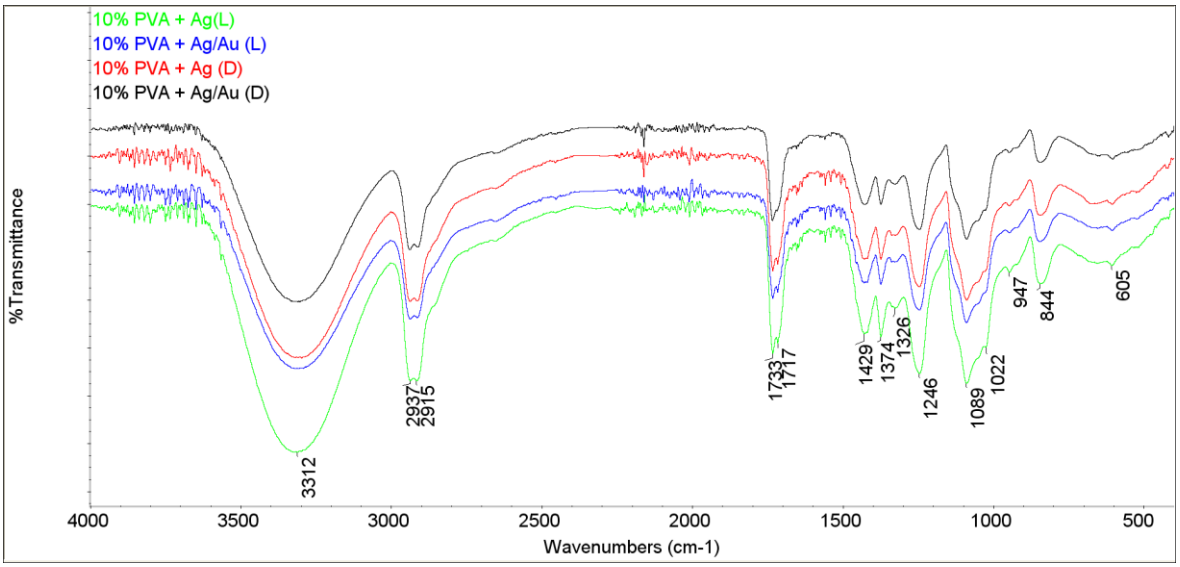

Figure 27: FTIR spectra of PVA fibers prepared using electrostatic spinning

Furthermore, 10 % PVA with incorporated powder bionanocomposites were measured. Figure 28 describes structural arrangement of these samples. Bands corresponded to fiber origin of poly(vinyl alcohol) samples as was mentioned above, were also presented in the FTIR spectra as well as bands associated with diatomic powder bionanocomposites. Thus, FTIR analysis confirmed a presence of bionanocomposite in fibrous sample.

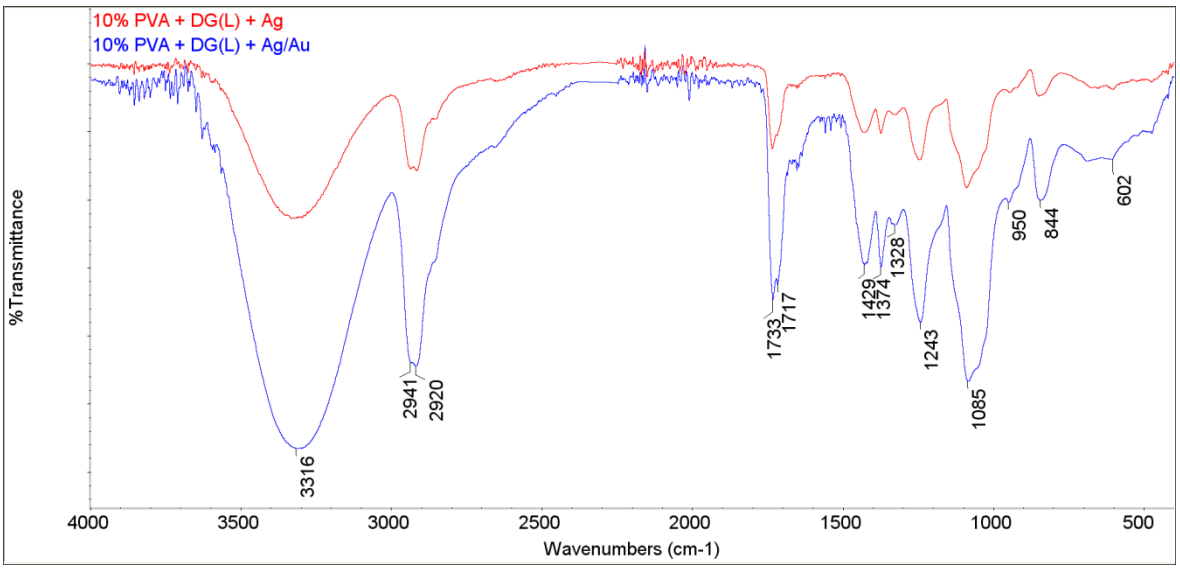

Figure 28: FTIR spectra of PVA fibers with powder bionanocomposite inside

4.5 Evaluation of spinning effectiveness

Centrifugal spinning performed in Pardam company provided PVA/NPs fibrous samples. From this type of spinning process the weight of prepared fibers was between 0.1818 g to 0.2817 g which is sufficient for laboratory testing processes. For centrifugal spinning 24 % wt of PVA polymer solution was recommended. During optimization process about 10 pieces of PVA/NPs fibers were prepared using different spinning speeds (see Appendix). According to the acquired knowledge, 7000 rpm was determined for these types of polymer fibers with metallic nanoparticles inside. Following table summarizes information about samples formed at rotational speed 7000 rpm.

Table 7: A summary of PVA/NPs samples prepared by centrifugal spinning at 7000 rpm

Sample	V[3] (mL)	m[4] (g)	t[5] (min)
24% PVA + Ag(L)	2	0.2817	2x10
24% PVA + Ag/Au(L)	2	0.2067	3x10
24% PVA + Ag(D)	2	0.1880	3x10
24% PVA + Ag/Au(D)	2	0.1818	3x10

Electrostatic spinning (Nanospider^{TM} technique) was also an effective way to fiber preparation. Unlike centrifugal spinning the electrostatic spinning gives samples with larger specimen size in laboratory conditions (about 20 x 100 cm). As well as a centrifugal spinning, Nanospider technique is suitable method for small volume fibrous material production and for commercial issues too [153, 154].

[3] V = volume of injected polymer solution into the spinneret
[4] m = final weight of prepared fibrous samples
[5] t = time cycle recommended for sample preparation

Figure 29: PVA fibers (a white film) deposited on a spunbond

Both methods have advantages and drawbacks. After centrifugal spinning process, the fibers were collected on the metallic collector arranged in the circle. Some amount of fibers remained on the metal collector which led to the sample shrinkage. Nanospider technique provided an almost profitable process however some amount of polymer may rest inside the spinning unit.

In the term of manipulating and working process, centrifugal spinning was easy and effective and did not take a long time to prepare a sample. In the case of electrostatic spinning method, a manipulation with spinning machine during electrostatic process required an experience and practice. Moreover, a presence of high voltage in the machine requires a compliance with safety rules. According to an optimization process the morphology of spun fibers may be adjusted to research purposes.

Only nanoparticle colloidal solutions were suitable for centrifugal process (see Figure 30). The limitation was a size of diatom frustules moving in the order of micrometers. Diatom size was too large to enable an extension of viscous jet through a needle. On the contrary, Nanospider machine was needleless technique and diatom frustules may fell to a collector together with fibers. Therefore, both colloidal solutions and powder sample were suitable. Diatom bodies are on the surface of fibers because the diameter of fibers is several times smaller than frustules.

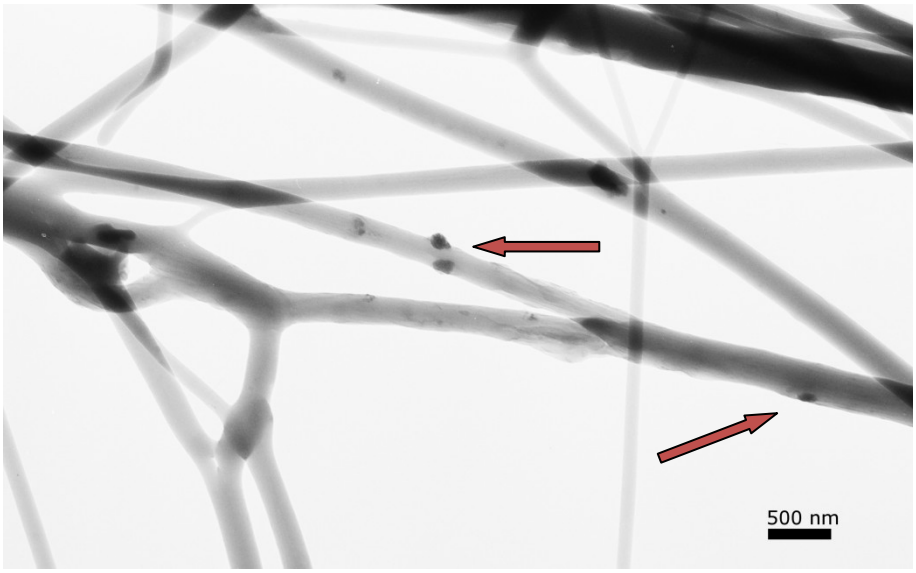

Figure 30: Colloidal nanoparticles incorporated into the PVA fibers; Ag(L) sample, centrifugal spinning

From centrifugal spinning method, the fibers are torn (Figure 31) and many defects were present in the form of the beads. The appearance of the fibers was significantly influenced by the spinning process including an optimization of the rotation speed and polymer solution concentration.

On the other hand, electrostatic spinning also influenced on the overall appearance of the fibers (Figure 32). Despite the fact that the fiber was not homogeneously spread, fibers were not excessively curled. In addition, the fiber diameter seems to be uniform in contrast to fibers prepared using centrifugal spinning.

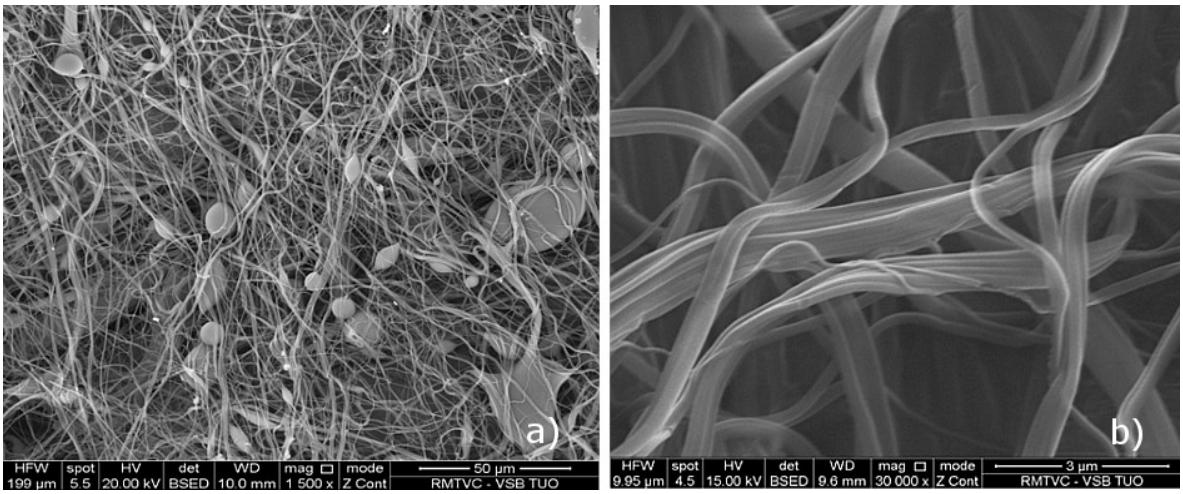

Figure 31: SEM micrographs of PVA fibers prepared by centrifugal spinning: picture a) PVA fibers containing Ag/Au(L) colloid, b) PVA fiber containing Ag(L) colloid

Special fiber morphology was observed after spinning process, e.g. two or more fibers appeared to be connected to one. Thicker fibers led to their own separation, producing finer fibers, but the “rope” profile still remained.

Average diameters of polymer fibers were completely different according to the way of spinning. In the case of electrospinning process, diameters ranged between 200 and 300 nm with occasional presence of lower diameter values. On the other hand, centrifugal spinning provided larger diameters. Determination of average diameter was difficult due to non–homogeneous structural arrangement with high number of defects. Polymer fibers obtained from centrifugal spinning disposed of diameters in the range of 500 – 1000 nm.

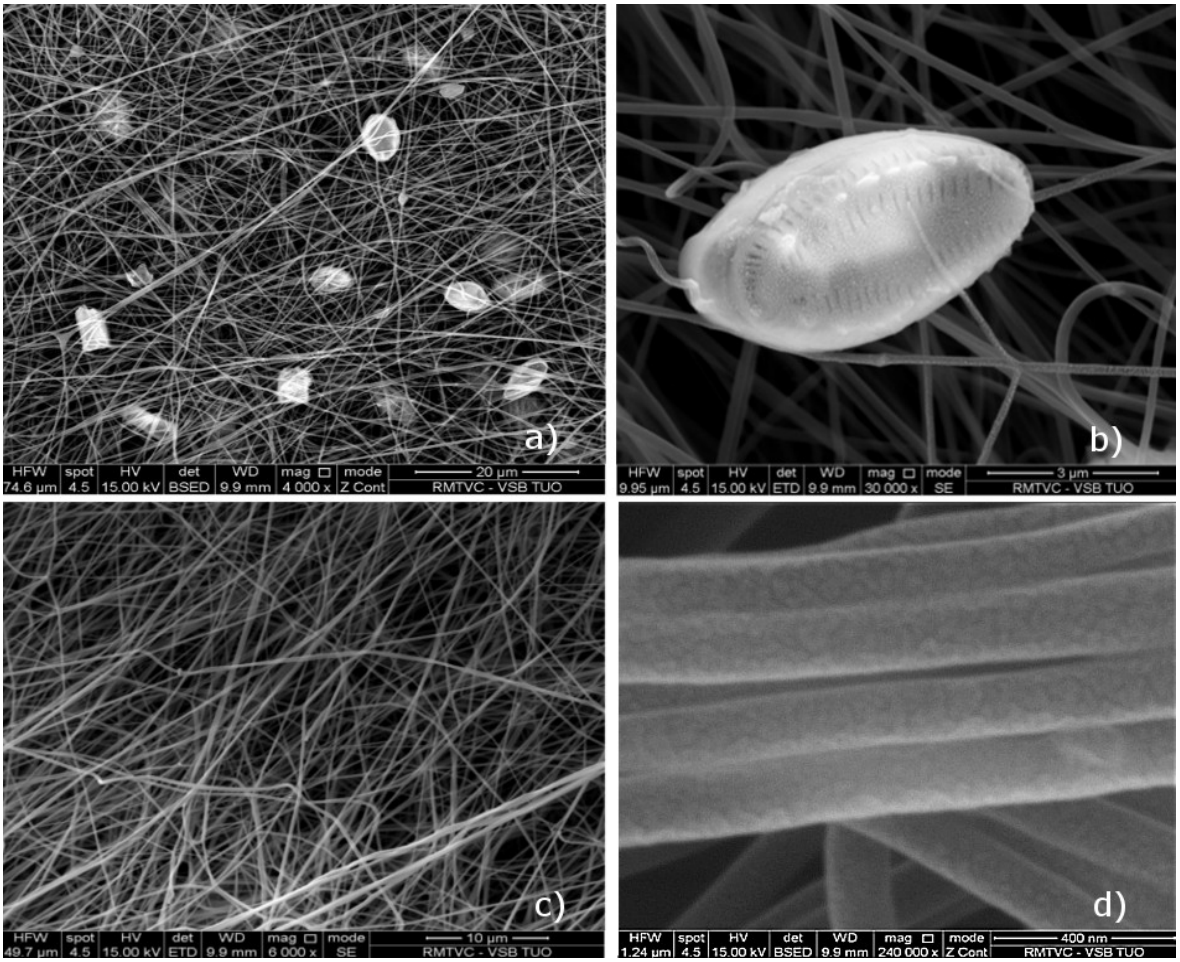

Figure 32: SEM micrographs of PVA fibers prepared by electrostatic spinning: a)-b) fibers containing diatom frustules, DG(L)Ag/Au sample; c)-d) fibers contain colloidal solutions, a presence of nanoparticles is not obvious, Ag(L) sample

Prepared fibers with nanoparticles have several drawbacks for future application research. Water-solubility of PVA may be undesirable in many applications. In the case of protective fibrous membrane in the respirator fiber coatings they can be dissolved due to moisture from breathing. Moreover, fiber breathability should be evaluated.

Due to this reason, polymer material should be changed in the future experiments. However type of polymer fibers is closely linked with the prepared nanoparticles. Because biosynthesized nanoparticles are dispersed in aqueous solution, for preliminary tests of fiber preparation a water-soluble polymer such as PVA was chosen.

Nanoparticles can be converted into another solvent, e.g. to ethanol, to provide polymer fibers resistant to the moisture. The question is how nanoparticles can be converted without significant loss. An effective centrifugation may help [155, 156] however nanoparticles may not be in ideal form because of a possible degradation or aggregation.

In conclusion electrospinning was more effective to produce polymer fibers with biosynthesized nanoparticles. Electrospun fibers were smooth with representative values of their diameters. Furthermore, diatom frustules may attach on the fibers surface as well as nanoparticles from colloidal solutions. This fact can lead to a preparation of new promising hybrid nanocomposite maybe used in medicine or in protective equipments such as breathing respirators.

4.6 Antibacterial evaluation

Four types of bionanocomposites were tested using MIC testing. According to previous research [38, 145, 157-160] silver nanoparticles exhibited antibacterial properties against wide range of bacteria cultures. Based on electrostatic interactions the nanoparticles may attach to the cell wall of bacteria and initiate the oxidative stress caused by the occurrence of free radicals [159]. A general term of free radicals includes superoxide radicals, hydroxyl radicals, hydrogen peroxide radicals and the singlet oxygen. After an initiation of free radicals formation, a destruction of the cellular components can start [161, 162]. Therefore free radicals cause the disruption of cell wall integrity and cell components, which contribute to cell death [159].

Studies dealing with the antibacterial activity usually worked with both gram-positive and gram-negative bacteria. In antibacterial testing a frequently used gram-positive bacteria are families of *Micrococcaceae* (e.g. *Staphylococcus aureu*s [163-167]) or *Bacillaceae* (e.g. *Bacillus subtilis* [167-170]). In the case of gram-negative bacteria widely utilized cultures are family of *Enterobacteraceae* where *Escherichia coli* (*E. coli*) belongs or *Pseudomonadaceae* with *Pseumonas aeruginosa* [38, 167, 171-173] .

Recently, researchers explored antibacterial properties not only of silver nanoparticles [53, 144, 174], but also of gold nanoparticles [141, 143, 144]. Not only nanoparticles synthesized by chemical method showed antibacterial effects, but green synthesized nanoparticles may be used as antibacterial agents too. This point is very important to an investigation of antimicrobial properties of biosynthesized nanoparticles. For example gold spherical nanoparticles (synthesized with extract of *Ananascomosus*) in average size of 16 nm showed antibacterial properties against *Staphylococcus aureus* (*S. aureus*) and *Pseudomonas aeruginosa* [141]. Another plant extract (from *Solanum nigrum*) is suitable for gold nanoparticles synthesis with antibacterial properties against gram-positive *Staphylococcus saprophyticus*, *Bacillus subtilis* and gram-negative *Pseudomonas aeruginosa* and *E.coli* [143]. An antibacterial assessment of silver and gold nanoparticles was compared in the presence of *S. aureus*, *E.coli* or *Proteus vulgaris*. Both types of nanoparticles showed bactericidal effects against aforementioned bacteria [175].

In this work an antibacterial testing was tasked with confirmation of antibacterial properties of silver nanoparticles and combination of silver and gold nanoparticles biosynthesized with *Diadesmis gallica*. For antibacterial tests these bacterial strains were

chosen: gram-positive *S. aureus*, *Streptococcus agalactiae* and *Bacillus cereus*; gram- negative *E. coli* and *Pseudomonas aeruginosa*.

According to obtained data bionanocomposites DG(L)Ag and DG(D)Ag disposed of similar trends. Sample with 1.12 % wt. of Ag bionanocomposite did not show antibacterial effects after first 24 hours in any of selected bacterial cultures (Table 8 and Table 9).

Table 8: MIC of DG(L)Ag bionanocomposite, SET1

Day		**1**			**2**			**3**		
Concentration (% wt.)		**1.12**	**3.3**	**10**	**1.12**	**3.3**	**10**	**1.12**	**3.3**	**10**
Type of composite	**Bacteria culture**									
DG(L)Ag	*Bacillus cereus*									
	Staphylococcus aureus									
	Streptococcus agalactiae									
	Escherichia coli									
	Pseudomonas aeruginosa									

Negative Slowing down 100% inhibition

Table 9: MIC of DG(D)Ag bionanocomposite, SET 1

Day		**1**			**2**			**3**		
Concentration (% wt.)		**1.12**	**3.3**	**10**	**1.12**	**3.3**	**10**	**1.12**	**3.3**	**10**
Type of composite	**Bacteria culture**									
DG(D)Ag	*Bacillus cereus*									
	Staphylococcus aureus									
	Streptococcus agalactiae									
	Escherichia coli									
	Pseudomonas aeruginosa									

After the second day of incubation the bionanocomposites showed slow inhibition of bacterial growth at *E. coli*. The rest of bacteria cultures grew without any changes. The antibacterial effects were changed after third day of incubation. Samples showed

antibacterial properties against gram-negative *E. coli* and gram-positive *B. cereus* and *S. aureus*.

Significant differences occurred at 3.3. % wt and 10 % wt of bionanocomoposite sample. Sample with 3.3 % wt and 10 % wt showed effective antibacterial properties than 1.2 % wt samples after 24 hours. As it is well seen from Table 5 and Table 6 a slowing down of all bacteria growth except *Pseudomonas aeruginosa* was visible after second day.

Third day of bacteria incubation in the presence of biosynthesized silver nanoparticles bring the most representative results. The most significant effects were visible at both gram positive and gram-negative bacteria where inhibition of bacterial growth became. Moreover the slowing inhibition was also detected at *Pseudomonas aeruginosa* which is the most resistant bacteria from used strains. One considerable difference between DG(L)Ag and DG(D)Ag was an inhibition of cell growth after 48 hours at DG(L)Ag at aforementioned *Pseudomonas aeruginosa*.

Despite a lower amount of silver nanoparticles in DG(L)Ag sample showed comparable results as a sample with dead diatomic cells. According to TEM analysis DG(L)Ag had a higher amount of nanoparticles in size between 6 - 9 nm and they may easily penetrate to the cell.

Generally, three gram-positive bacteria and gram-negative *E. coli* were not resistant against silver nanoparticles activity. Only *P. aeruginosa* showed strong resistance disposition against the 10 % wt concentrations of bionanocomposites. This may be caused by different requirements for living condition of *P. aeruginosa*; *S. aureus* and *E. coli* may be more sensitive to changes in living conditions. *P. aeruginosa* showed the lowest sensitivity against from bacteria used in antibacterial evaluation. Bacterial cells may have some defense mechanism which can help them to resist the treatment of used samples or other chemicals [176].

Bionanocomposites with silver and gold combination were tested. The similar trends as in the case of silver samples were observed with one difference (Table 10 and Table 11). Unlike DG(D)Ag, DG(L)Ag/Au and DG(D)Ag/Au samples also showed antibacterial effect against *P. aeruginosa* after 48 hours.

Table 10: MIC of DG(L)Ag/Au sample, SET 1

Day		1			2			3		
Concentration (% wt.)		1.12	3.3	10	1.12	3.3	10	1.12	3.3	10
Type of composite	Bacteria culture									
DG(L)Ag/Au	*Bacillus cereus*									
	Staphylococcusaureus									
	Streptococcus agalactiae									
	Escherichia coli									
	Pseudomonas aeruginosa									

Negative Slowing down 100% inhibition

Table 11: MIC of DG(L)Ag/Au sample, SET 1

Day		1			2			3		
Concentration (% wt.)		1.12	3.3	10	1.12	3.3	10	1.12	3.3	10
Type of composite	Bacteria culture									
DG(D)Ag/Au	*Bacillus cereus*									
	Staphylococcusaureus									
	Streptococcus agalactiae									
	Escherichia coli									
	Pseudomonas aeruginosa									

This type of antibacterial evaluation confirmed antibacterial properties of silver nanoparticles as well as gold nanoparticles. But it is not easy to determine how large amount of gold was participated in antibacterial effect. Gold may have synergistic effect with silver and may support its antibacterial properties.

Colloidal solutions were also analyzed. The amount of silver and both silver and gold nanoparticles were not enough to obtain a relevant antibacterial effectiveness. In the silver nanoparticle solutions the amount of metals was recalculated to ppm unit. Nanoparticle concentrations were 11.3, 9.7 and 11.9 ppm. In commercial polymer fibers with antibacterial properties, the amount of silver was from 50 to 200 ppm [177]. Thus the

amount of active nanoparticles is not high enough and it may be the reason why antibacterial effects were not confirmed.

PVA fibers with incorporated bionanocomposites inside were also tested using disc diffusion test. Two types of fiber membranes were tested to verify the antibacterial properties. In both samples diatomic composites containing silver nanoparticles or a combination of silver and gold nanoparticles were incorporated.

For antibacterial testing, three bacterial cultures were chosen such as *E. coli*, *P. aeruginosa* and *S. aureus*. Results of this antibacterial evaluation could not be accurately interpreted as a disc diffusion test. The disc diffusion test is based on the antibacterial agent (antibiotics, nanoparticles) penetration to its surroundings and affects on the bacterial culture growth on the agar plate. The bacterial inhibition is indicated as clear zones without bacterial film around the agent. The diameter of these zones increases with concentration of chosen agent [178].

In this case an inhibition of bacterial growth was due to direct contact of the fibrous sample. Water soluble PVA fibrous membrane was dissolved under the influence of agar moisture. However, the active compound in the form of bionanocomposite was released and showed bactericidal effects alongside the shape of fibrous membrane. In the case of *E. coli* and *P. aeruginosa* the results were clearly visible (Figure 33). Fiber membrane containing silver nanoparticles showed strong antibacterial activity against aforementioned cultures. In the case of a combination of metals the antibacterial activity was not so high however, growth of bacterial cultures was inhibited.

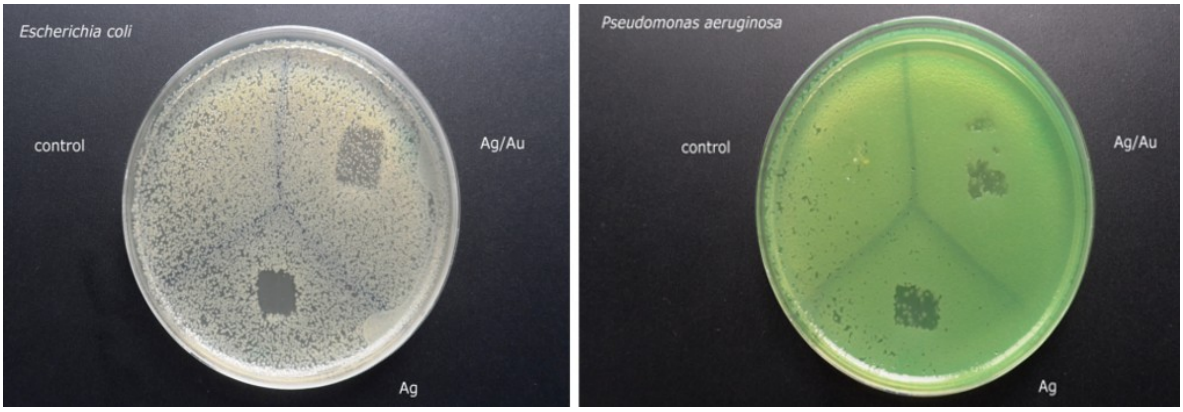

Figure 33: The bacterial growth inhibition areas against gram – negative bacteria *E. coli* and *P. aeruginosa*

Antibacterial test of gram-positive *S. aureus* showed different behavior compared to previous results. Dissolution of fibrous sample was not clearly seen (Figure 34). Moreover

a number of bacteria cultures grew on the place of fiber membrane. This feature may be caused by the non-homogeneous distribution of nanoparticles inside the fibers.

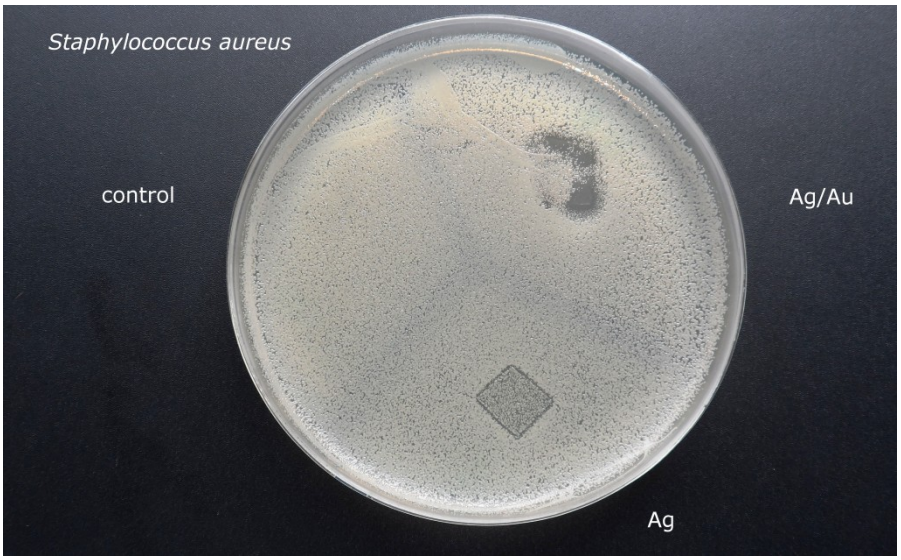

Figure 34: Antibacterial activity of fibrous samples against gram-positive *S. aureus*

In conclusion, biosynthesized silver and both silver and gold nanoparticles showed antibacterial activity against chosen bacteria cultures. The most effective concentration of bionanocomposite in MIC evaluation was 10 % wt of used sample. This concentration caused 100 % inhibition of bacterial growth except *Streptococcus agalactiae* and *P. aeruginosa.* The combination of silver and gold nanoparticles did not show higher antibacterial effectiveness than silver nanoparticles. According to the ICP-AES results gold may contribute to antibacterial effects because an amount of silver was smaller than gold. Thus, gold may took over the role of a major antibacterial agent in these types of samples.

Colloidal solutions of nanoparticles did not showed any antibacterial effects because of low amount of active antibacterial agent.

Polymer fibers with incorporated bionanocomposites (from living biomass) contributed to antibacterial activity. The assumption of effective antibacterial properties of fibrous membranes was based on representative MIC results. Despite the bionanocomposites inside the fibers were spread at the large sample area, antibacterial properties of electrospun hybrid composite were noticeable. This may be a promising beginning of incorporation process of biosynthesized nanoparticles into the fiber membrane with special properties.

5. CONCLUSIONS

This master thesis is divided in two parts – Theoretical and Experimental part. Theoretical part may be considered as a comprehensive literature review focused on three main topics such as preparation of silver and gold nanoparticles via biosynthesis, incorporation of metallic nanoparticles into polymer fibers and future applications of these hybrid nanocomposites.

Brief overview of basic biosynthesis principles clarify a synthesis of metallic nanoparticles used in various applications such as medicine, wound dressings or filtration systems.

Metal nanoparticles have a great potential to be incorporated into the polymer fibers. Literature review of the spinning techniques such as centrifugal spinning and electrospinning was also included. Both methods had advantages and drawbacks however optimization process may enhance final properties of polymer fibers. Last chapter of Theoretical part dealt with applications of incorporated nanoparticles in various types of polymers. Different polymer fibers were described with regard to Experimental part. Moreover, applications of PVA and metal nanoparticles were included.

Experimental part described an incorporation of silver and gold nanoparticles in the PVA polymer fibers step by step. First, silver and gold nanoparticles were prepared via biosynthesis using brown algae *Diadesmis gallica*. Silver nanoparticles and combination of silver and gold nanoparticles were prepared in two different forms. First was the powder bionanocomposite containing diatom silica frustules with attached nanoparticles. The second one - colloidal solution - was obtained during bionanocomposite preparation.

For both spinning methods colloidal solutions were suitable. Colloidal solutions were mixed with PVA and then spun via centrifugal spinning and electrospinning. Optimization of spinning processes was required to obtain representative fibers. Nanoparticles from colloids were attached on the fiber surface. Unlike centrifugal spinning electrospinning process was suitable method for incorporation of powder bionanocomposites. With respect to silica frustules sizes diatoms were attached on the surface of polymer fibers.

According to previous results in the field of silver and both silver and gold nanoparticles antibacterial evaluation was performed. In the case of silver and gold combination antibacterial effectiveness was higher than silver nanoparticles agent [30]. In this work, this phenomenon was not confirmed probably due to unbalanced amount of silver and gold nanoparticles. However, in this experiment antibacterial properties was

confirmed at silver and both silver and gold nanoparticles. Moreover, PVA fibers with diatom bionanocomposite inside showed antibacterial effectiveness too. PVA fibers with incorporated nanoparticles and diatom frustules may serve as a new hybrid nanocomposite used for example in protective equipment such as respirator.

6. REFERENCES

1. Schrödinger, E., *Science and humanism; physics in our time*. 1951, Cambridge Eng.: University Press. 68 p.
2. Feynman, R. *There's Plenty of Room at the Bottom: An Invitation to Enter a New Field of Physics.* 1959; Available from: http://www.zyvex.com/nanotech/feynman.html.
3. Iijima, S., *Helical microtubules of graphitic carbon.* Nature, 1991. 354(6348): p. 56-58.
4. Sakka, S., *Sol-Gel Technology as Reflected in Journal of Sol-Gel Science and Technology.* Journal of Sol-Gel Science and Technology, 2003. 26(1-3): p. 29-33.
5. Fert, A., et al., *Giant Magnetoresistance of (001)Fe/(001)Cr Magnetic Superlattices.* Physical Review Letters, 1988. 61(21): p. 2472-2475.
6. Drude, P., C.R. Mann, and R.A. Millikan, *The Theory of optics*, in *Nineteenth Century Collections Online (NCCO): Science, Technology, and Medicine: 1780-1925*. 1902, Longmans, Green, and Co.,: New York ; London. p. 1 online resource (1 , xxi, 546 p.).
7. Chopra, K.L., *Thin film phenomena*. 1969, New York: McGraw-Hill. xx, 844 p.
8. Chaloupka, K., Y. Malam, and A.M. Seifalian, *Nanosilver as a new generation of nanoproduct in biomedical applications.* Trends in biotechnology, 2010. 28(11): p. 580-588.
9. Alanazi, F.K., A.A. Radwan, and I.A. Alsarra, *Biopharmaceutical applications of nanogold.* Saudi Pharmaceutical Journal, 2010. 18(4): p. 179-193.
10. de Vargas, I., L.E. Macaskie, and E. Guibal, *Biosorption of palladium and platinum by sulfate-reducing bacteria.* Journal of Chemical Technology & Biotechnology, 2004. 79(1): p. 49-56.
11. *National Nanotechnology Initiative*. 2004; Available from: http://www.nano.gov/.
12. Krahne, R., et al., *Physical properties of elongated inorganic nanoparticles.* Physics Reports, 2011. 501(3–5): p. 75-221.
13. Son, Y., et al., *Application of the specific thermal properties of Ag nanoparticles to high-resolution metal patterning.* Thermochimica Acta, 2012. 542(0): p. 52-56.
14. Díez-Pascual, A.M., et al., *Mechanical and electrical properties of carbon nanotube/poly(phenylene sulphide) composites incorporating polyetherimide and inorganic fullerene-like nanoparticles.* Composites Part A: Applied Science and Manufacturing, 2012. 43(4): p. 603-612.
15. Narayanan, K.B. and N. Sakthivel, *Biological synthesis of metal nanoparticles by microbes.* Advances in Colloid and Interface Science, 2010. 156(1–2): p. 1-13.
16. *Manufacturing at the Nanoscale*. 2015; Available from: http://www.nano.gov/nanotech-101/what/manufacturing.
17. Hübsch, C., et al., *Protection of yttria-stabilized zirconia for dental applications by oxidic PVD coating.* Acta Biomaterialia, 2015. 11(0): p. 488-493.
18. Fujioka, H., *8 - Pulsed Laser Deposition (PLD)*, in *Handbook of Crystal Growth (Second Edition)*, T.F. Kuech, Editor. 2015, North-Holland: Boston. p. 365-397.
19. Mereu, R.A., et al., *Comparative study on structural, morphological and optical properties of Zn2SnO4 thin films prepared by r.f. sputtering using Zn and Sn metal targets and ZnO–SnO2 ceramic target.* Journal of Alloys and Compounds, 2015. 626(0): p. 112-117.
20. Omri, A., M. Benzina, and F. Bennour, *Industrial application of photocatalysts prepared by hydrothermal and sol–gel methods.* Journal of Industrial and Engineering Chemistry, 2015. 21(0): p. 356-362.

21. Junlabhut, P., et al., *Characterization of ZnO:Sn Nanopowders Synthesized by Co-precipitation Method.* Energy Procedia, 2014. 56(0): p. 560-565.
22. Simha Martynková, G., et al., *Structural ordering of organovermiculite: Experiments and modeling.* Journal of Colloid and Interface Science, 2007. 313(1): p. 281-287.
23. Filipová, Z., et al., *Biosyntéza nanomateriálů*. 2012, Olomouc: Univerzita Palackého v Olomouci. 63.
24. Schröfel, A., et al., *Biosynthesis of gold nanoparticles using diatoms—silica-gold and EPS-gold bionanocomposite formation.* Journal of Nanoparticle Research, 2011. 13(8): p. 3207-3216.
25. Castro-Longoria, E., A.R. Vilchis-Nestor, and M. Avalos-Borja, *Biosynthesis of silver, gold and bimetallic nanoparticles using the filamentous fungus Neurospora crassa.* Colloids and Surfaces B: Biointerfaces, 2011. 83(1): p. 42-48.
26. Rajakumar, G., et al., *Fungus-mediated biosynthesis and characterization of TiO2 nanoparticles and their activity against pathogenic bacteria.* Spectrochimica Acta Part a-Molecular and Biomolecular Spectroscopy, 2012. 91: p. 23-29.
27. Zhang, W., et al., *Biosynthesis and structural characteristics of selenium nanoparticles by Pseudomonas alcaliphila.* Colloids Surf B Biointerfaces, 2011. 88(1): p. 196-201.
28. Zhang, X., et al., *Synthesis of nanoparticles by microorganisms and their application in enhancing microbiological reaction rates.* Chemosphere, 2011. 82(4): p. 489-94.
29. Schröfel, A., *Biosynthesis of metallic nanoparticles and their applications*, in *Faculty of Metallurgy and Materials Engineering*. 2012, VŠB-Technical University of Ostrava: . p. 101.
30. Konvičková, Z., *Antimikrobiální vlastnosti biosyntetizovaných kovových nanočástic s pomocí hnědých řas*, in *Centrum nanotechnologií*. 2013, Vysoká škola báňská - Technická univerzita Ostrava: Ostrava. p. 52.
31. Natšinová, M., *Příprava a charakterizace zlatých nanočástic a studium jejich katalytické aktivity*, in *Centrum nanotechnologií*. 2014, Vysoká škola báňská - Technická univerzita Ostrava: Ostrava.
32. Holišová, V., *Hydrolýza bojových látek s využtiím biosyntetizovaných zlatých nanočástic*, in *Centrum nanotechnologií*. 2014, Vysoká škola báňská - Technická Univerzita Ostrava: Ostrava.
33. Kalina, T. and J. Váňa, *Sinice, řasy, houby, mechorosty a podobné organismy v současné biologii*. 2005, Praha: Karolinum.
34. Holišová, V., *Biosyntéza nanočástic ušlechtilých kovů*, in *University Study Programmes*. 2012, VŠB - Technical Universtity od Ostrava. p. 39.
35. Rajasree, S.R.R. and T.Y. Suman, *Extracellular biosynthesis of gold nanoparticles using a gram negative bacterium Pseudomonas fluorescens.* Asian Pacific Journal of Tropical Disease, 2012. 2, Supplement 2(0): p. S796-S799.
36. Malhotra, A., et al., *Biosynthesis of gold and silver nanoparticles using a novel marine strain of Stenotrophomonas.* Bioresource Technology, 2013. 142(0): p. 727-731.
37. Anand, B.G., et al., *Biosynthesis of silver nano-particles by marine sediment fungi for a dose dependent cytotoxicity against HEp2 cell lines.* Biocatalysis and Agricultural Biotechnology, (0).
38. Singh, D., et al., *Biosynthesis of silver nanoparticle by endophytic fungi Pencillium sp. isolated from Curcuma longa (turmeric) and its antibacterial activity against*

pathogenic gram negative bacteria. Journal of Pharmacy Research, 2013. 7(5): p. 448-453.
39. Sharma, B., et al., *Biosynthesis of gold nanoparticles using a freshwater green alga, Prasiola crispa.* Materials Letters, 2014. 116(0): p. 94-97.
40. Senapati, S., et al., *Intracellular synthesis of gold nanoparticles using alga Tetraselmis kochinensis.* Materials Letters, 2012. 79(0): p. 116-118.
41. Luna, C., et al., *Biosynthesis of silver fine particles and particles decorated with nanoparticles using the extract of Illicium verum (star anise) seeds.* Spectrochimica Acta Part A: Molecular and Biomolecular Spectroscopy, 2015. 141(0): p. 43-50.
42. Mittal, A.K., et al., *Biosynthesis of silver nanoparticles: Elucidation of prospective mechanism and therapeutic potential.* Journal of Colloid and Interface Science, 2014. 415(0): p. 39-47.
43. LÜ, F., et al., *Roles of Biomolecules in the Biosynthesis of Silver Nanoparticles: Case of Gardenia jasminoides Extract.* Chinese Journal of Chemical Engineering, 2014. 22(6): p. 706-712.
44. Durán, N., et al., *Antibacterial Effect of Silver Nanoparticles Produced by Fungal Process on Textile Fabrics and Their Effluent Treatment.* Journal of Biomedical Nanotechnology, 2007. 3(2): p. 203-208.
45. Kratošová, G., et al., *Synthesis of Metallic Nanoparticles by Diatoms - Prospect and Applications*, in *Green biosynthesis of nanoparticles: mechanisms and applications.*, M. Rai and C. Posten, Editors. 2013, CABI Publishing: UK. p. 256.
46. Vijayaraghavan, K., et al., *Biosynthesis of Au(0) from Au(III) via biosorption and bioreduction using brown marine alga Turbinaria conoides.* Chem Eng J, 2011. 167(1): p. 5-5.
47. Ponnuchamy, K., *Synthesis of silver nanoparticles from Sargassum tenerrimum and screening phytochemicals for its anti-bacterial activity.* Nano Biomedicine, 2012. 4(1): p. 12-16.
48. Mata, Y.N., et al., *Gold(III) biosorption and bioreduction with the brown alga Fucus vesiculosus.* Journal of Hazardous Materials, 2009. 166(2–3): p. 612-618.
49. Zhou, Y., et al., *Biosynthesis of Gold Nanoparticles by Foliar Broths: Roles of Biocompounds and Other Attributes of the Extracts.* Nanoscale Research Letters, 2010. 5(8): p. 1351-1359.
50. Bar, H., et al., *Green synthesis of silver nanoparticles using latex of Jatropha curcas.* Colloids and Surfaces A: Physicochemical and Engineering Aspects, 2009. 339(1–3): p. 134-139.
51. Martínková, L., et al., *Biodegradation potential of the genus Rhodococcus.* Environment International, 2009. 35(1): p. 162-177.
52. Otari, S.V., et al., *Intracellular synthesis of silver nanoparticle by actinobacteria and its antimicrobial activity.* Spectrochimica Acta Part A: Molecular and Biomolecular Spectroscopy, 2015. 136, Part B(0): p. 1175-1180.
53. Otari, S.V., et al., *Green synthesis of silver nanoparticles by microorganism using organic pollutant: its antimicrobial and catalytic application.* Environmental Science and Pollution Research, 2014. 21(2): p. 1503-1513.
54. Chronakis, I.S., *Novel nanocomposites and nanoceramics based on polymer nanofibers using electrospinning process—A review.* Journal of Materials Processing Technology, 2005. 167(2–3): p. 283-293.
55. Sebe, I., et al., *Polymer structure and antimicrobial activity of polyvinylpyrrolidone-based iodine nanofibers prepared with high-speed rotary spinning technique.* International Journal of Pharmaceutics, 2013. 458(1): p. 99-103.

56. Nair, L.S. and C.T. Laurencin, *Biodegradable polymers as biomaterials.* Progress in Polymer Science, 2007. 32(8–9): p. 762-798.
57. McMurry, J., *Organic chemistry*. 6th ed. 2004, Belmont, CA: Thomson-Brooks/Cole.
58. *Book Review of What is What in the Nanoworld: A Handbook on Nanoscience and Nanotechnology, Completely Revised and Enlarged 2nd ed.* Journal of the American Chemical Society, 2008. 130(50): p. 17204-17204.
59. Alfrey, T. and E.F. Gurnee, *Organic polymers*. Prentice-Hall series in materials science. 1967, Englewood Cliffs, N.J.,: Prentice-Hall. ix, 131 p.
60. Kulkarni, S., *Robust Process Development and Scientific Molding - Theory and Practice*. Hanser Publishers.
61. Mleziva J., K.J., *Základy makromolekulární chemie*. 1. ed. 1986, Praha: SNTL - Nakladatelství technické literatury. 384.
62. Ross, K.A., S.D. Arntfield, and S. Cenkowski, *A Polymer Science Approach to Physico-Chemical Characterization and Processing of Pulse Seeds*. Polymer Science. 2013.
63. Roos, Y.H., *Glass Transition Temperature and Its Relevance in Food Processing.* Annual Review of Food Science and Technology, 2010. 1(1): p. 469-496.
64. Sperling, L.H., *Introduction to physical polymer science*. 4th ed. 2006, Hoboken, N.J.: Wiley-Interscience. xxx, 845 p.
65. Slade, L. and H. Levine, *Beyond water activity: recent advances based on an alternative approach to the assessment of food quality and safety.* Crit Rev Food Sci Nutr, 1991. 30(2-3): p. 115-360.
66. Huang, Z.-M., et al., *A review on polymer nanofibers by electrospinning and their applications in nanocomposites.* Composites Science and Technology, 2003. 63(15): p. 2223-2253.
67. Lukáš, D., et al., *Physical principles of electrospinning (Electrospinning as a nano-scale technology of the twenty-first century).* Textile Progress, 2009. 41(2): p. 59-140.
68. Sung, Y.K., B.W. Ahn, and T.J. Kang, *Magnetic nanofibers with core (Fe3O4 nanoparticle suspension)/sheath (poly ethylene terephthalate) structure fabricated by coaxial electrospinning.* Journal of Magnetism and Magnetic Materials, 2012. 324(6): p. 916-922.
69. Barakat, N.A.M., B. Kim, and H.Y. Kim, *Production of Smooth and Pure Nickel Metal Nanofibers by the Electrospinning Technique: Nanofibers Possess Splendid Magnetic Properties.* The Journal of Physical Chemistry C, 2009. 113(2): p. 531-536.
70. Andrady, A.L., *Science and Technology of Polymer Nanofibers*. 1st ed. 2008: Wiley - Interscience. 404 p.
71. Gwinn, R.P., *The New Encyclopedia Britannica*. Vol. 5. 1991, Chicago: Encyclopedia Britannica Inc.
72. Morton, W.J., *Method of dispersing fluids*. 1902, Google Patents.
73. Zeleny, J., *The Electrical Discharge from Liquid Points, and a Hydrostatic Method of Measuring the Electric Intensity at Their Surfaces.* Physical Review, 1914. 3(2): p. 69-91.
74. Ruska, E., *The early development of electron lenses and electron microscopy*. 1980, Stuttgart: Hirzel. 140 p.
75. Jirsak, O., et al., *Method of nanofibres production from a polymer solution using electrostatic spinning and a device for carrying out the method*. 2009, Google Patents.

76. Wilm, M.S. and M. Mann, *Electrospray and Taylor-Cone theory, Dole's beam of macromolecules at last?* International Journal of Mass Spectrometry and Ion Processes, 1994. 136(2–3): p. 167-180.
77. Bhardwaj, N. and S.C. Kundu, *Electrospinning: A fascinating fiber fabrication technique.* Biotechnology Advances, 2010. 28(3): p. 325-347.
78. Reneker, D.H. and A.L. Yarin, *Electrospinning jets and polymer nanofibers.* Polymer, 2008. 49(10): p. 2387-2425.
79. Erben, J., et al., *The combination of meltblown and electrospinning for bone tissue engineering.* Materials Letters, 2015. 143(0): p. 172-176.
80. Zhang, Y.Z., et al., *Characterization of the surface biocompatibility of the electrospun PCL-collagen nanofibers using fibroblasts.* Biomacromolecules, 2005. 6(5): p. 2583-9.
81. Zhang, C., et al., *Study on morphology of electrospun poly(vinyl alcohol) mats.* European Polymer Journal, 2005. 41(3): p. 423-432.
82. Li, W.-J., et al., *Electrospun nanofibrous structure: A novel scaffold for tissue engineering.* Journal of Biomedical Materials Research, 2002. 60(4): p. 613-621.
83. Li, M., et al., *Electrospun protein fibers as matrices for tissue engineering.* Biomaterials, 2005. 26(30): p. 5999-6008.
84. Kenawy, E.-R., et al., *Release of tetracycline hydrochloride from electrospun poly(ethylene-co-vinylacetate), poly(lactic acid), and a blend.* Journal of Controlled Release, 2002. 81(1–2): p. 57-64.
85. Ho, B.-C., Y.-D. Lee, and W.-K. Chin, *Thermal degradation of polymethacrylic acid.* Journal of Polymer Science Part A: Polymer Chemistry, 1992. 30(11): p. 2389-2397.
86. Bamford, C.H., et al., *Studies of a novel membrane for affinity separations: I. Functionalisation and protein coupling.* Journal of Chromatography A, 1992. 606(1): p. 19-31.
87. KAUR, S., et al., *OLIGOSACCHARIDE FUNCTIONALIZED NANOFIBROUS MEMBRANE.* International Journal of Nanoscience, 2006. 05(01): p. 1-11.
88. Reneker, D.H., et al., *Nanofiber garlands of polycaprolactone by electrospinning.* Polymer, 2002. 43(25): p. 6785-6794.
89. Doshi, J. and D.H. Reneker, *Electrospinning process and applications of electrospun fibers.* Journal of Electrostatics, 1995. 35(2–3): p. 151-160.
90. Ahn, Y.C., et al., *Development of high efficiency nanofilters made of nanofibers.* Current Applied Physics, 2006. 6(6): p. 1030-1035.
91. Chiu, H., et al., *Fabrication of electrospun polyacrylonitrile ion-exchange membranes for application in lysozym.* Express Polymer Letters, 2011. 5(4): p. 308-317.
92. Zhang, Y.Z., et al., *Crosslinking of the electrospun gelatin nanofibers.* Polymer, 2006. 47(8): p. 2911-2917.
93. Jia, J., et al., *Preparation and Characterization of Antibacterial Silver-containing Nanofibers for Wound Dressing Applications.* Journal of US-China Medical Science, 2007. 4(2): p. 52-54.
94. Byoung Chan, K., et al., *Preparation of biocatalytic nanofibres with high activity and stability via enzyme aggregate coating on polymer nanofibres.* Nanotechnology, 2005. 16(7): p. S382.
95. Ramakrishna, S., et al., *Electrospun nanofibers: solving global issues.* Materials Today, 2006. 9(3): p. 40-50.

96. *Poly(ethylene/vinyl acetate) [72:28 (wt)]*. 2015; Available from: http://www.polysciences.com/default/catalog-products/monomers-polymers/polymers/poly-eva-poly-evoh/polyethylenevinyl-acetate-7228-wt/.
97. Mellado, P., et al., *A simple model for nanofiber formation by rotary jet-spinning.* Applied Physics Letters, 2011. 99(20): p. -.
98. Sarkar, K., et al., *Electrospinning to Forcespinning™.* Materials Today, 2010. 13(11): p. 12-14.
99. Lu, Y., et al., *Parameter study and characterization for polyacrylonitrile nanofibers fabricated via centrifugal spinning process.* European Polymer Journal, 2013. 49(12): p. 3834-3845.
100. Leventon, W. *Spin controlled: Texas company offers improved way to spin nanofibers*. 2013; Available from: http://www.micromanufacturing.com/content/spin-controlled-texas-company-offers-improved-way-spin-nanofibers.
101. Chang, W.-M., C.-C. Wang, and C.-Y. Chen, *The combination of electrospinning and forcespinning: Effects on a viscoelastic jet and a single nanofiber.* Chemical Engineering Journal, 2014. 244(0): p. 540-551.
102. McEachin, Z. and K. Lozano, *Production and characterization of polycaprolactone nanofibers via forcespinning™ technology.* Journal of Applied Polymer Science, 2012. 126(2): p. 473-479.
103. Ren, L., R. Ozisik, and S.P. Kotha, *Rapid and efficient fabrication of multilevel structured silica micro-/nanofibers by centrifugal jet spinning.* Journal of Colloid and Interface Science, 2014. 425(0): p. 136-142.
104. Ren, L., et al., *Large-scale and highly efficient synthesis of micro- and nano-fibers with controlled fiber morphology by centrifugal jet spinning for tissue regeneration.* Nanoscale, 2013. 5(6): p. 2337-2345.
105. Mary, L.A., et al., *Centrifugal spun ultrafine fibrous web as a potential drug delivery vehicle.* Express Polymer Letters, 2013. 7(3): p. 238-248.
106. Shanmuganathan, K., et al., *Solventless High Throughput Manufacturing of Poly(butylene terephthalate) Nanofibers.* ACS Macro Letters, 2012. 1(8): p. 960-964.
107. Qiao, B., et al., *Study on the Electrospun CNTs/Polyacrylonitrile-Based Nanofiber Composites.* Journal of Nanomaterials, 2011. 2011: p. 7.
108. Wang, L., et al., *Fabrication of polymer fiber scaffolds by centrifugal spinning for cell culture studies.* Microelectronic Engineering, 2011. 88(8): p. 1718-1721.
109. Ren, L. and S.P. Kotha, *Centrifugal jet spinning for highly efficient and large-scale fabrication of barium titanate nanofibers.* Materials Letters, 2014. 117(0): p. 153-157.
110. Lu, Y., et al., *Centrifugal spinning: A novel approach to fabricate porous carbon fibers as binder-free electrodes for electric double-layer capacitors.* Journal of Power Sources, (0).
111. Deniz, A.E., et al., *Gold nanoparticle/polymer nanofibrous composites by laser ablation and electrospinning.* Materials Letters, 2011. 65(19–20): p. 2941-2943.
112. Virovska, D., et al., *Electrospinning/electrospraying vs. electrospinning: A comparative study on the design of poly(l-lactide)/zinc oxide non-woven textile.* Applied Surface Science, 2014. 311(0): p. 842-850.
113. Fathona, I.W. and A. Yabuki, *Short electrospun composite nanofibers: Effects of nanoparticle concentration and surface charge on fiber length.* Current Applied Physics, 2014. 14(5): p. 761-767.

114. Salalha, W., et al., *Single-walled carbon nanotubes embedded in oriented polymeric nanofibers by electrospinning.* Langmuir, 2004. 20(22): p. 9852-5.
115. Hansen, L.M., et al., *Water absorption and mechanical properties of electrospun structured hydrogels.* Journal of Applied Polymer Science, 2005. 95(2): p. 427-434.
116. He, D., et al., *Large-scale synthesis of flexible free-standing SERS substrates with high sensitivity: electrospun PVA nanofibers embedded with controlled alignment of silver nanoparticles.* ACS Nano, 2009. 3(12): p. 3993-4002.
117. Wang, Y., et al., *Preparation of silver nanoparticles dispersed in polyacrylonitrile nanofiber film spun by electrospinning.* Materials Letters, 2005. 59(24–25): p. 3046-3049.
118. More, D.S., et al., *TOPO-capped silver selenide nanoparticles and their incorporation into polymer nanofibers using electrospinning technique.* Materials Research Bulletin, 2015. 65(0): p. 14-22.
119. Song, T., Y.Z. Zhang, and T.J. Zhou, *Fabrication of magnetic composite nanofibers of poly(ε-caprolactone) with FePt nanoparticles by coaxial electrospinning.* Journal of Magnetism and Magnetic Materials, 2006. 303(2): p. e286-e289.
120. Jeon, H.J., et al., *Preparation of poly(ε-caprolactone)-based polyurethane nanofibers containing silver nanoparticles.* Applied Surface Science, 2008. 254(18): p. 5886-5890.
121. Nguyen, T.H., et al., *Nano Ag loaded PVA nano-fibrous mats for skin applications.* J Biomed Mater Res B Appl Biomater, 2011. 96(2): p. 225-33.
122. Xu, X., et al., *Biodegradable electrospun poly(l-lactide) fibers containing antibacterial silver nanoparticles.* European Polymer Journal, 2006. 42(9): p. 2081-2087.
123. Nguyen, T.-H., K.-H. Lee, and B.-T. Lee, *Fabrication of Ag nanoparticles dispersed in PVA nanowire mats by microwave irradiation and electro-spinning.* Materials Science and Engineering: C, 2010. 30(7): p. 944-950.
124. Zhao, Y., et al., *A facile method for electrospinning of Ag nanoparticles/poly (vinyl alcohol)/carboxymethyl-chitosan nanofibers.* Applied Surface Science, 2012. 258(22): p. 8867-8873.
125. Hadipour-Goudarzi, E., et al., *Electrospinning of chitosan/sericin/PVA nanofibers incorporated with in situ synthesis of nano silver.* Carbohydrate Polymers, 2014. 113(0): p. 231-239.
126. Pencheva, D., R. Bryaskova, and T. Kantardjiev, *Polyvinyl alcohol/silver nanoparticles (PVA/AgNps) as a model for testing the biological activity of hybrid materials with included silver nanoparticles.* Materials Science and Engineering: C, 2012. 32(7): p. 2048-2051.
127. Yu, A.K., et al., *Synthesis and properties of silver nanoparticles: advances and prospects.* Russian Chemical Reviews, 2008. 77(3): p. 233.
128. Shahi, M., et al., *Electrospun PVA–PANI and PVA–PANI– composite nanofibers.* Scientia Iranica, 2011. 18(6): p. 1327-1331.
129. Celebioglu, A., et al., *One-step synthesis of size-tunable Ag nanoparticles incorporated in electrospun PVA/cyclodextrin nanofibers.* Carbohydrate Polymers, 2014. 99(0): p. 808-816.
130. Wisniak, J., *Thomas Graham. II. Contributions to diffusion of gases and liquids, colloids, dialysis, and osmosis.* Educación Química, 2013. 24, Supplement 2(0): p. 506-515.

131. Clariant GmbH. ®*Mowiol Polyvinyl Alcohol*. 1999; Available from: http://www2.cbm.uam.es/confocal/Manuales/mowiol.pdf.
132. PRWeb. *FibeRio Wins R&D 100 Award for Nanofiber Production Equipment, Launches Third Product* 2014; Available from: http://ww1.prweb.com/prfiles/2011/07/05/8622439/L1000D_Final.jpg.
133. Okutan, N., P. Terzi, and F. Altay, *Affecting parameters on electrospinning process and characterization of electrospun gelatin nanofibers.* Food Hydrocolloids, 2014. 39(0): p. 19-26.
134. Elmarco. *Nanospider Production Line NS 1WS500U*. Available from: http://www.elmarco.com/upload/soubory/dokumenty/141-1-ns-1ws500u-profile-111004-72dpi.pdf.
135. Pabst W., G.E., *Charakterizace částic a částicových soustav*. 2007, Praha: VŠCHT Praha. 110.
136. Holešová, S., et al., *Preparation of novel organovermiculites with antibacterial activity using chlorhexidine diacetate.* Journal of Colloid and Interface Science, 2010. 342(2): p. 593-597.
137. Rooij, A.d. *The Oxidation of Silver by Atomic Oxyge*. 1989 [cited 13; ESA Journal:[363]. Available from: http://esmat.esa.int/Atox_on_Ag.PDF.
138. Bock, F.X., et al., *Growth and structure of silver and silver oxide thin films on sapphire.* Thin Solid Films, 2004. 468(1–2): p. 57-64.
139. Gao, X., et al., *Effects of hydrogen annealing on the microstructure and optical properties of single-phased Ag2O film deposited using direct-current reactive magnetron sputtering.* Thin Solid Films, 2011. 519(19): p. 6620-6623.
140. Leonard, K., et al., *In situ green synthesis of biocompatible ginseng capped gold nanoparticles with remarkable stability.* Colloids and Surfaces B: Biointerfaces, 2011. 82(2): p. 391-396.
141. Bindhu, M.R. and M. Umadevi, *Antibacterial activities of green synthesized gold nanoparticles.* Materials Letters, 2014. 120(0): p. 122-125.
142. Guerra, R., E. Lima, and A. Guzmán, *Antimicrobial supported nanoparticles: Gold versus silver for the cases of Escherichia coli and Salmonella typhi.* Microporous and Mesoporous Materials, 2013. 170(0): p. 62-66.
143. Muthuvel, A., et al., *Biosynthesis of gold nanoparticles using Solanum nigrum leaf extract and screening their free radical scavenging and antibacterial properties.* Biomedicine & Preventive Nutrition, 2014. 4(2): p. 325-332.
144. Naraginti, S. and A. Sivakumar, *Eco-friendly synthesis of silver and gold nanoparticles with enhanced bactericidal activity and study of silver catalyzed reduction of 4-nitrophenol.* Spectrochim Acta A Mol Biomol Spectrosc, 2014. 128: p. 357-62.
145. Gopinath, V., et al., *Biosynthesis of silver nanoparticles from Tribulus terrestris and its antimicrobial activity: A novel biological approach.* Colloids and Surfaces B: Biointerfaces, 2012. 96(0): p. 69-74.
146. *WebElements Periodic Table: the periodic table on the web*. Available from: http://www.webelements.com/.
147. Kim, G.-M., *Fabrication of Bio-Nanocomposite Nanofibers Mimicking the Mineralized Hard Tissues via Electrospinning Process*. 2010.
148. Clayden, J., *Organic chemistry*. 2008, Oxford ; New York: Oxford University Press. 1512 p.

149. Khanna, P.K., et al., *Synthesis and characterization of Ag/PVA nanocomposite by chemical reduction method.* Materials Chemistry and Physics, 2005. 93(1): p. 117-121.
150. Ali, I.O., *Synthesis and characterization of Ag0/PVA nanoparticles via photo- and chemical reduction methods for antibacterial study.* Colloids and Surfaces A: Physicochemical and Engineering Aspects, 2013. 436(0): p. 922-929.
151. Priya, B., et al., *Synthesis, characterization and antibacterial activity of biodegradable starch/PVA composite films reinforced with cellulosic fibre.* Carbohydrate Polymers, 2014. 109(0): p. 171-179.
152. Li, N., et al., *Preparation and properties of PVDF/PVA hollow fiber membranes.* Desalination, 2010. 250(2): p. 530-537.
153. Elmarco. *Produkty*. Available from: http://www.elmarco.cz/produkty/produkty/.
154. Fiberio. *Fiber Engine® FX*. Available from: http://fiberiotech.com/products/industrial-equipment/fiberengine-fx/.
155. Lee, S., B. Salunke, and B. Kim, *Sucrose density gradient centrifugation separation of gold and silver nanoparticles synthesized using Magnolia kobus plant leaf extracts.* Biotechnology and Bioprocess Engineering, 2014. 19(1): p. 169-174.
156. Akbulut, O., et al., *Separation of Nanoparticles in Aqueous Multiphase Systems through Centrifugation.* Nano Letters, 2012. 12(8): p. 4060-4064.
157. Zhu, Z.-C., et al., *One-step synthesis and antibacterial property of water-soluble silver nanoparticles by CGJ bio-template.* Journal of Nanoparticle Research, 2011. 13(10): p. 5347-5353.
158. Zargar, M., et al., *Green Synthesis and Antibacterial Effect of Silver Nanoparticles Using Vitex Negundo L.* Molecules, 2011. 16(8): p. 6667-6676.
159. Hajipour, M.J., et al., *Antibacterial properties of nanoparticles.* Trends in biotechnology, 2012. 30(10): p. 499-511.
160. Marambio-Jones, C. and E.V. Hoek, *A review of the antibacterial effects of silver nanomaterials and potential implications for human health and the environment.* Journal of Nanoparticle Research, 2010. 12(5): p. 1531-1551.
161. Votava, M., *Lékařská mikrobiologie obecná*. 2001, Brno: Neptun. 247.
162. You, C., et al., *The progress of silver nanoparticles in the antibacterial mechanism, clinical application and cytotoxicity.* Molecular Biology Reports, 2012. 39(9): p. 9193-9201.
163. Shirley, et al., *Antimicrobial activity of silver nanoparticles synthesized from novel Streptomyces species.* Digest Journal of Nanomaterials and Biostructures, 2010. 5(2): p. 447-451.
164. Nithya, R. and R. Ragunathan, *Synthesis of silver nanoparticle using Pleurotus saju cajo and its antimicrobial study.* Digest Journal of Nanomaterials and Biostructures, 2009. 4(4): p. 623-629.
165. Veerasamy, R., et al., *Biosynthesis of silver nanoparticles using mangosteen leaf extract and evaluation of their antimicrobial activities.* Journal of Saudi Chemical Society, 2011. 15(2): p. 113-120.
166. Nabikhan, A., et al., *Synthesis of antimicrobial silver nanoparticles by callus and leaf extracts from saltmarsh plant, Sesuvium portulacastrum L.* Colloids and Surfaces B-Biointerfaces, 2010. 79(2): p. 488-493.
167. Musarrat, J., et al., *Production of antimicrobial silver nanoparticles in water extracts of the fungus Amylomyces rouxii strain KSU-09.* Bioresource Technology, 2010. 101(22): p. 8772-8776.
168. Suresh, A.K., et al., *Silver Nanocrystallites: Biofabrication using Shewanella oneidensis, and an Evaluation of Their Comparative Toxicity on Gram-negative*

and Gram-positive Bacteria. Environmental Science & Technology, 2010. 44(13): p. 5210-5215.
169. Sadhasivam, S., P. Shanmugam, and K. Yun, *Biosynthesis of silver nanoparticles by Streptomyces hygroscopicus and antimicrobial activity against medically important pathogenic microorganisms.* Colloids and Surfaces B-Biointerfaces, 2010. 81(1): p. 358-362.
170. Saha, S., et al., *Production of silver nanoparticles by a phytopatogenic fungus Bipolaris nodulosa and its antimicrobial activity.* Digest Journal of Nanomaterials and Biostructures, 2010. 5(4): p. 887-895.
171. Prasad, T. and E.K. Elumalai, *Biofabrication of Ag nanoparticles using Moringa oleifera leaf extract and their antimicrobial activity.* Asian Pacific Journal of Tropical Biomedicine, 2011. 1(6): p. 439-442.
172. Dar, M.A., A. Ingle, and M. Rai, *Enhanced antimicrobial activity of silver nanoparticles synthesized by Cryphonectria sp. evaluated singly and in combination with antibiotics.* Nanomedicine: Nanotechnology, Biology and Medicine, 2013. 9(1): p. 105-110.
173. Maliszewska, I. and M. Puzio, *Extracellular Biosynthesis and Antimicrobial Activity of Silver Nanoparticles.* Acta Physica Polonica A, 2009. 116: p. S160-S162.
174. Puišo, J., et al., *Biosynthesis of silver nanoparticles using lingonberry and cranberry juices and their antimicrobial activity.* Colloids and Surfaces B: Biointerfaces, 2014. 121(0): p. 214-221.
175. R, G. and S. D.V.L, *Characterization and antimicrobial activity of gold and silver nanoparticles synthesized using saponin isolated from Trianthema decandra L.* Industrial Crops and Products, 2013. 51(0): p. 107-115.
176. Dědková, K., et al., *Preparation, characterization and antibacterial properties of ZnO/kaoline nanocomposites.* Journal of Photochemistry and Photobiology B: Biology, 2015. 148(0): p. 113-117.
177. Pardam. *Polymer nanofibrous membranes, NnF MBRANE® – PVB (Polyvinylbutyral)*. Available from: http://pardam.cz/products/?wpcproduct=nnf-mbrane-pvb.
178. Bonev, B., J. Hooper, and J. Parisot, *Principles of assessing bacterial susceptibility to antibiotics using the agar diffusion method.* Journal of Antimicrobial Chemotherapy, 2008. 61(6): p. 1295-1301.

APPENDIX

The results of the statistical particle size evaluation in DG (L)Ag sample

i	x_i (nm)	n_i	$q_0(x_i)$	$q_0(x_i)$ (%)	$x_i \cdot n_i$ (nm)	$(x_i - \bar{x}_A)^2$ $(nm)^2$	$q_0(x_i) \cdot (x_i - \bar{x}_A)^2$ $(nm)^2$
1	0.000	0.000	0.000	0.000	0.000	295.398	0.000
2	3.000	4.000	0.011	1.117	12.000	201.275	2.249
3	**6.000**	**75.000**	0.209	**20.950**	450.000	125.152	26.219
4	**9.000**	**107.000**	0.299	**29.888**	963.000	67.029	20.034
5	12.000	58.000	0.162	16.201	696.000	26.907	4.359
6	15.000	17.000	0.047	4.749	255.000	4.784	0.227
7	18.000	8.000	0.022	2.235	144.000	0.661	0.015
8	21.000	8.000	0.022	2.235	168.000	14.538	0.325
9	24.000	5.000	0.014	1.397	120.000	46.415	0.648
10	27.000	8.000	0.022	2.235	216.000	96.292	2.152
11	30.000	3.000	0.008	0.838	90.000	164.169	1.376
12	33.000	6.000	0.017	1.676	198.000	250.046	4.191
13	36.000	8.000	0.022	2.235	288.000	353.923	7.909
14	39.000	6.000	0.017	1.676	234.000	475.800	7.974
15	42.000	11.000	0.031	3.073	462.000	615.677	18.917
16	45.000	6.000	0.017	1.676	270.000	773.555	12.965
17	48.000	6.000	0.017	1.676	288.000	949.432	15.912
18	51.000	4.000	0.011	1.117	204.000	1 143.309	12.774
19	54.000	5.000	0.014	1.397	270.000	1 355.186	18.927
20	57.000	2.000	0.006	0.559	114.000	1 585.063	8.855
21	60.000	4.000	0.011	1.117	240.000	1 832.940	20.480
22	63.000	2.000	0.006	0.559	126.000	2 098.817	11.725
23	66.000	2.000	0.006	0.559	132.000	2 382.694	13.311
24	69.000	2.000	0.006	0.559	138.000	2 684.571	14.998
25	72.000	0.000	0.000	0.000	0.000	3 004.448	0.000
26	75.000	1.000	0.003	0.279	75.000	3 342.326	9.336
27	78.000	0.000	0.000	0.000	0.000	3 698.203	0.000
Σ	**-**	**358.000**	**1.000**	**100.000**	**6 153.000**	**-**	**235.878**

The results of the statistical particle size evaluation in DG(L)Ag/Au sample

i	x_i (nm)	n_i	$q_0(x_i)$	$q_0(x_i)$ (%)	$x_i \cdot n_i$ (nm)	$(x_i - \bar{x}_A)^2$ $(nm)^2$	$q_0(x_i) \cdot (x_i - \bar{x}_A)^2$ $(nm)^2$
1	0.000	1.000	0.004	0.360	0.000	401.152	1.443
2	**3.000**	**49.000**	0.176	**17.626**	147.000	289.979	51.111
3	**6.000**	**68.000**	0.245	**24.460**	408.000	196.807	48.140
4	9.000	12.000	0.043	4.317	108.000	121.634	5.250
5	12.000	4.000	0.014	1.439	48.000	64.461	0.928
6	15.000	5.000	0.018	1.799	75.000	25.289	0.455
7	18.000	7.000	0.025	2.518	126.000	4.116	0.104
8	21.000	12.000	0.043	4.317	252.000	0.943	0.041
9	24.000	15.000	0.054	5.396	360.000	15.771	0.851
10	27.000	20.000	0.072	7.194	540.000	48.598	3.496
11	30.000	8.000	0.029	2.878	240.000	99.425	2.861
12	33.000	15.000	0.054	5.396	495.000	168.253	9.078
13	36.000	12.000	0.043	4.317	432.000	255.080	11.011
14	39.000	18.000	0.065	6.475	702.000	359.907	23.303
15	42.000	6.000	0.022	2.158	252.000	482.735	10.419
16	45.000	4.000	0.014	1.439	180.000	623.562	8.972
17	48.000	7.000	0.025	2.518	336.000	782.389	19.700
18	51.000	4.000	0.014	1.439	204.000	959.217	13.802
19	54.000	4.000	0.014	1.439	216.000	1154.044	16.605
20	57.000	1.000	0.004	0.360	57.000	1366.871	4.917
21	60.000	2.000	0.007	0.719	120.000	1597.699	11.494
22	63.000	2.000	0.007	0.719	126.000	1846.526	13.284
23	66.000	0.000	0.000	0.000	0.000	2113.353	0.000
24	69.000	0.000	0.000	0.000	0.000	2398.181	0.000
25	72.000	2.000	0.007	0.719	144.000	2701.008	19.432
26	75.000	0.000	0.000	0.000	0.000	3021.835	0.000
27	78.000	0.000	0.000	0.000	0.000	3360.663	0.000
Σ	-	**278.000**	**1.000**	**100.000**	**5568.000**	-	**276.697**

The results of the statistical particle size evaluation in DG(D)Ag sample

i	x_i (nm)	n_i	$q_0(x_i)$	$q_0(x_i)$ (%)	$x_i \cdot n_i$ (nm)	$(x_i - \bar{x}_A)^2$ $(nm)^2$	$q_0(x_i) \cdot (x_i - \bar{x}_A)^2$ $(nm)^2$
1	0.000	0.000	0.000	0.000	0.000	490.648	0.000
2	3.000	25.000	0.071	7.102	75.000	366.744	2604.718
3	**6.000**	**39.000**	0.111	**11.080**	234.000	260.841	2889.998
4	9.000	25.000	0.071	7.102	225.000	172.937	1228.249
5	12.000	27.000	0.077	7.670	324.000	103.034	790.318
6	**15.000**	**34.000**	0.097	**9.659**	510.000	51.131	493.875
7	18.000	22.000	0.063	6.250	396.000	17.227	107.670
8	21.000	25.000	0.071	7.102	525.000	1.324	9.402
9	24.000	25.000	0.071	7.102	600.000	3.420	24.293
10	27.000	22.000	0.063	6.250	594.000	23.517	146.981
11	30.000	18.000	0.051	5.114	540.000	61.614	315.069
12	33.000	24.000	0.068	6.818	792.000	117.710	802.569
13	36.000	11.000	0.031	3.125	396.000	191.807	599.396
14	39.000	14.000	0.040	3.977	546.000	283.903	1129.161
15	42.000	11.000	0.031	3.125	462.000	394.000	1231.250
16	45.000	10.000	0.028	2.841	450.000	522.097	1483.229
17	48.000	3.000	0.009	0.852	144.000	668.193	569.483
18	51.000	3.000	0.009	0.852	153.000	832.290	709.338
19	54.000	3.000	0.009	0.852	162.000	1014.386	864.534
20	57.000	4.000	0.011	1.136	228.000	1214.483	1380.094
21	60.000	4.000	0.011	1.136	240.000	1432.579	1627.931
22	63.000	1.000	0.003	0.284	63.000	1668.676	474.056
23	66.000	1.000	0.003	0.284	66.000	1922.773	546.242
24	69.000	0.000	0.000	0.000	0.000	2194.869	0.000
25	72.000	1.000	0.003	0.284	72.000	2484.966	705.956
26	75.000	0.000	0.000	0.000	0.000	2793.062	0.000
27	78.000	0.000	0.000	0.000	0.000	3119.159	0.000
Σ	**-**	**352.000**	**1.000**	**100.000**	**7797.000**	**-**	**20733.812**

The results of the statistical particle size evaluation in DG(D)Ag /Au sample

i	x_i (nm)	n_i	$q_0(x_i)$	$q_0(x_i)$ (%)	$x_i \cdot n_i$ (nm)	$(x-\bar{x}_A)^2$ $(nm)^2$	$q_0(x_i)\cdot(x_i-\bar{x}_A)^2$ $(nm)^2$
1	0.000	0.000	0.000	0.000	0.000	71.701	0.000
2	3.000	85.000	0.141	14.096	255.000	29.895	4.214
3	**6.000**	**220.000**	0.365	**36.484**	1320.000	6.089	2.222
4	**9.000**	**146.000**	0.242	**24.212**	1314.000	0.283	0.069
5	12.000	79.000	0.131	13.101	948.000	12.477	1.635
6	15.000	44.000	0.073	7.297	660.000	42.671	3.114
7	18.000	11.000	0.018	1.824	198.000	90.865	1.658
8	21.000	11.000	0.018	1.824	231.000	157.060	2.865
9	24.000	4.000	0.007	0.663	96.000	241.254	1.600
10	27.000	2.000	0.003	0.332	54.000	343.448	1.139
11	30.000	1.000	0.002	0.166	30.000	463.642	0.769
12	33.000	0.000	0.000	0.000	0.000	601.836	0.000
13	36.000	0.000	0.000	0.000	0.000	758.030	0.000
14	39.000	0.000	0.000	0.000	0.000	932.224	0.000
15	42.000	0.000	0.000	0.000	0.000	1124.418	0.000
16	45.000	0.000	0.000	0.000	0.000	1334.612	0.000
17	48.000	0.000	0.000	0.000	0.000	1562.806	0.000
18	51.000	0.000	0.000	0.000	0.000	1809.000	0.000
19	54.000	0.000	0.000	0.000	0.000	2073.194	0.000
20	57.000	0.000	0.000	0.000	0.000	2355.388	0.000
21	60.000	0.000	0.000	0.000	0.000	2655.582	0.000
22	63.000	0.000	0.000	0.000	0.000	2973.776	0.000
23	66.000	0.000	0.000	0.000	0.000	3309.970	0.000
24	69.000	0.000	0.000	0.000	0.000	3664.164	0.000
25	72.000	0.000	0.000	0.000	0.000	4036.358	0.000
26	75.000	0.000	0.000	0.000	0.000	4426.552	0.000
27	78.000	0.000	0.000	0.000	0.000	4834.746	0.000
Σ	**-**	**603.000**	**1.000**	**100.000**	**5106.000**	**-**	**19.284**

The results of the statistical particle size evaluation in colloidal samples

Size range (nm)	Ag(L), SET 1 %	Ag/Au(L), SET 1 %	Ag(D), SET 1 %	Ag/Au(D), SET 1 %
0-10.100	0	0	0	0
10.100-12.700	0.45	0.16	0.39	0.01
12.7-16.000	0.83	0.78	1.52	0
16.000-20.100	1.73	2.11	3.49	0
20.100-25.200	3.58	4.22	6.87	0.2
25.200-31.700	7.03	8.35	11.61	2.58
31.700-39.900	14.08	15.06	19.59	8.31
39.900-50.200	**22.47**	22.9	**29.03**	20.33
50.200-63.100	**35.6**	**21.81**	**20.33**	**33.96**
63.100-79.300	11.09	**19.42**	5.05	**25.6**
79.300-99.700	1.98	3.98	0.93	7.88
Total particle weight (µg)	12.35	5.14	22.12	2.67

Optimization process of rotational speedsduring centrifugal spinning

Rotation speed	4500 rpm	5000 rpm	6000 rpm	6500 rpm	7000 rpm	V (ml)	m (g)	t (min)
Ag(L)	-	-	2 samples	-	2 samples	-	-	-
Ag/Au(L)	-	-	1 sample	1 sample	1 sample	-	-	-
Ag(D)	-	-	1 sample	-	-	3	-	3x10
		1 sample	-	-	-	2.2	0.2614	3x10
	1 sample	-	-	-	-	2	0.1925	3x10
Ag/Au(D)	-	1 sample	-	-	-	2	0.1395	3x10
	-	-	-	-	1 sample	2	0.2739	2x10